DESIGN OF A RADIOISOTOPE THERMO-PHOTOVOLTAIC POWER SOURCE BY LASER DRIVEN ISOTOPE SURROGATE ASSEMBLY

A Thesis

Presented in Partial Fulfillment of the Requirements for the

Degree of Master of Science

with a

Major in Mechanical Engineering

in the

College of Graduate Studies

University of Idaho

by

Troy Howe

December 2013

Major Professor: John Crepeau, Ph.D.

Authorization to Submit Thesis

This thesis of Troy Howe, submitted for the degree of Master of Science with a major in Mechanical Engineering and titled "Design of Radioisotope Thermo-Photovoltaic Power Source by Laser Driven Isotope Surrogate Assembly," has been reviewed in final form. Permission, as indicated by the signatures and dates given below, is now granted to submit final copies to the College of Graduate Studies for approval.

Major Professor	_____	Date_____
	Dr. John Crepeau	
Committee Members	_____	Date_____
	Dr. Raghunath Kanakala	
	_____	Date_____
	Dr. Judi Steciak	
Department Administrator	_____	Date_____
	Dr. John Crepeau	
Dean of the College of Engineering	_____	Date_____
	Dr. Larry Stauffer	

Final Approval and Acceptance by the College of Graduate Studies

_____Date_____

Dr. Jie Chen

Abstract

Thermo-photovoltaic (TPV) technologies have the potential to benefit a very important aspect of space exploration technology: the conversion of heat into electricity. A thermo-photovoltaic device uses a very hot source material which emits photons through radiative heat transfer and a photovoltaic (PV) cell to pick up that radiation to turn it into electricity via the photovoltaic effect [1]. The energy of emitted photons must match or surpass the band gap of the PV cell to function, and if properly tuned, quantum efficiencies of over 95% can be achieved [2]. A radioisotope thermo-photovoltaic (RTPV) uses a radioisotope as the heat source to achieve these high temperatures, as well as provide power over the course of decades. Given these potentially high efficiencies, long life spans, and lack of moving parts, RTPV technologies are ideal for space exploration situations where missions may take longer than 20 years to complete. Additionally, development in this area could contribute to alternative fuel cars [3], terrestrial power generation [4], or power sources in hostile environments.

The major aspects to investigate in TPV technology include the conductive heat losses through the mounting systems and the tuning of the emitter material to the PV band gap. For the heat loss aspect, a model was built in COMSOL and used to trace conductive losses through a model of an RTPV system. For the emissivity tuning aspect, facilities at the Idaho National Laboratory were used to develop a laser heated emissivity testing facility. The computer model was used to corroborate the experimental data and material properties, and an RTPV system was designed based on experimental results and computational modeling.

Based on the experimental data, the theoretical model would need to be much larger than initially planned to reach a functioning temperature. The emissivity of the tantalum emitter material increased with temperature, and the power input of the radioisotope source

was insufficient to keep temperatures high. Therefore, a larger power-to-emissive area was necessary. As the volume of the fuel rod increased, the emitting surface area also increased, but at a slower rate. So using more fuel would raise the maximum operating temperature.

The result of the project produced a testing device that could simulate a solid fuel power source for radioisotope thermophotovoltaic uses. Only a tantalum emitter surface was tested, but other materials could be used to improve emissive profiles in the future. Maximum testing temperatures reached 779 K, with optimized mounting systems and target properties. The final theoretical design was found to have external dimensions of 14.48 cm height by 12.7 cm diameter, not counting radiators. It used 1000 W of thermal power to generate 60W of electrical power, and reached a maximum temperature of 1200 K. This performance matched the efficiency and specific power of current thermoelectric generators. Further improvements to RTPV systems in the areas of selective emitters and maximum temperature increases will improve performance and make RTPV systems a preferred candidate for space power production.

Acknowledgements

I would like to the Dr. John Crepeau for his guidance and advice with this project, his encouragement during experimental challenges was a source of great inspiration and always kept the project on track and goal oriented.

I would also like to thank Dr. Carl M. Stoots, Dr. Robert C. O'Brien, and the Idaho National Lab for their contribution to the Laser Heating and Emissivity Experiments at the INL facilities.

Additionally I would like to thank the Center for Space Nuclear Research for creating and providing funding for this research project and all the people who made this work possible.

Dedication

Dedicated to Mom and Dad, who always provided a constant source of wisdom and encouragement, and are my greatest role models.

Table of Contents

List of Figures

List of Tables

Chapter 1: Introduction

1.0 Radioisotope Power Sources Overview

Radioisotope power sources are devices which are capable of providing electrical power to components for long periods of time by taking advantage of the natural heat released by a material due to radioactive decay. As a radioactive material decays, the subatomic bonds which hold nucleons or electrons in the atom break, and create kinetic energy in the form of moving particles [6]. These moving particles interact with other nearby particles, depositing energy and increasing temperatures. Converting the thermal energy that is generated by the radioisotopic decay into electrical power is the primary goal of a radioisotope power source. The major benefits of radioisotope power sources are their long life spans, robustness, and relatively small sizes. The major drawbacks are relatively low power levels, low temperatures and low efficiencies.

1.1 History of Radioisotope Power Sources

Radioisotope power sources have been used for some time, primarily on unmanned space missions, such as Voyager 1, Voyager 2, Galileo, and Curiosity, among others [7]. The most used radioisotope power source is known as the Radioisotope Thermoelectric Generator, or RTG. This device is constructed of plutonium oxide pellets inside layers of cladding and surrounded in a carbon shell. The shell can reach temperatures of 900-1,000 °C (1,173-1,273 K) [8], which provides enough of a temperature difference to provide power. While initial RTG's used spherical shaped heating units, in more recent times there has been a push to make a standardized design that could be used for multiple uses. Newer heating units retain the multiple layers of cladding, but contain four PuO_2 pellets each. The carbon shell around them is formed into a brick. These carbon covered bricks are referred to as General Purpose Heat

Sources, or GPHS units [9]. The three major RTG types are the original RTG, General Purpose Heat Source RTG (GPHS-RTG), and Multi Mission RTG (MMRTG). The original RTG on Voyager 1 and 2 used spherical heat sources, GPHS-RTGs used stacked together GPHS units in a tower to provide enough thermal power for a mission, and MMRTGs use a modified GHPS-RTG design to make a smaller unit capable of being used on a variety of missions. An exploded view of a GPHS unit is shown in Figure 1 below.

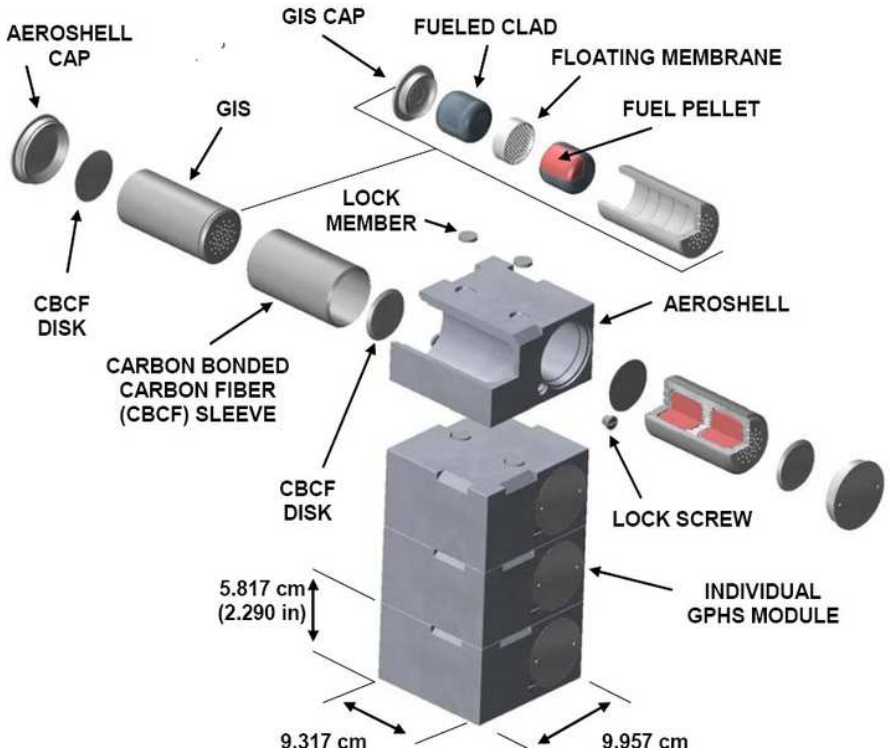

Figure 33: GPHS exploded view [9]

In an RTG unit, thermocouples which take advantage of the Seebeck effect are used to produce a voltage between two wires of dissimilar metals. That voltage can drive a circuit, and thus the RTG provides electrical power. In order to keep the largest temperature difference, and thus the highest voltage between wires, cooling fins are needed to radiate excess heat into space. These fins are added to the external surface of the RTG housing, increasing the overall size of the unit. An entire GPHS-RTG system occupies 0.20 cubic meters, has a height of 1.14

meters, a width of 0.42 meters, and a mass of 57kg. It is capable of providing 300 watts of electrical power at the beginning of its lifespan [10]. A GPHS RTG cutaway is seen in Figure 2.

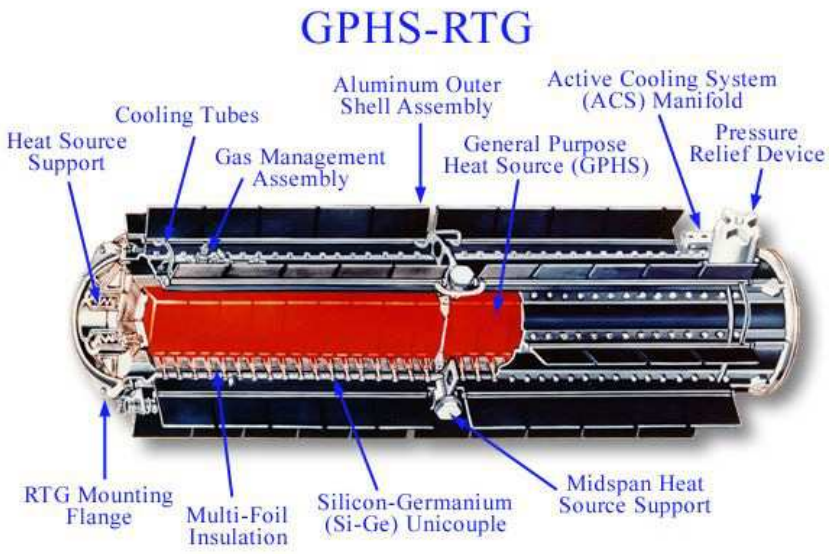

Figure 34: GPHS-RTG [9]

The MMRTG is the most modern RTG design, and was used on the recent unmanned mission to Mars by the Curiosity rover. It is the current technology used for radioisotope power and will be most often used as the comparison or baseline when comparing power source options. It provides less power than the GPHS-RTG, providing only 120 watts of electrical power per unit vs. the 300 watts of the GPHS-RTG, but it also has a lower mass of 43 kg than the 57 kg of the GHPS-RTG. Surprisingly, it has a higher volume at 0.27 cubic meters compared to the 0.20 cubic meters of the older unit. The efficiency is also lower, with the GPHS-RTG being near 6.8% efficient and the MMRTG at 6% [10], [7]. The benefit to the MMRTG is found in its standardized construction, rigorous flight testing and adaptability to different tasks. These tasks include the ability to function in the vacuum of space as well as within the atmosphere of a planet. Because the efficiency of the RTG is so low, there is ongoing research into other possible power production methods that could reduce waste heat, mass, and volume of the power source.

1.1.1 Other Options

The Advanced Stirling Radioisotope Generator (ASRG) is a power production device in development by NASA which is claimed to have higher conversion efficiency than the RTG devices [11]. It functions by using a Stirling engine attached to an electrical generator for power production. The Stirling engine concept relies on a moving piston alternating between a hot and cold side. In the starting position, the piston is fully extended and the working gas inside the chamber is at minimum volume. Because this position is in contact with a heat source, in this case a radioisotope, the gas heats up and begins to expand. That pushes the piston, which turns the generator and electrical power is produced. Once the piston passes a certain desired traveling distance, the hot gas escapes the piston assembly and flows to the heat rejection side, either by exposing a flow channel or using a displacer piston. When cooled, the gas reverts to its previous state. A flywheel or spring then continues the stroke of the piston rod, returning it to the original position. The cycle then begins again and continues until halted or the heat source diminishes [12]. Figure 3 shows a NASA Stirling converter.

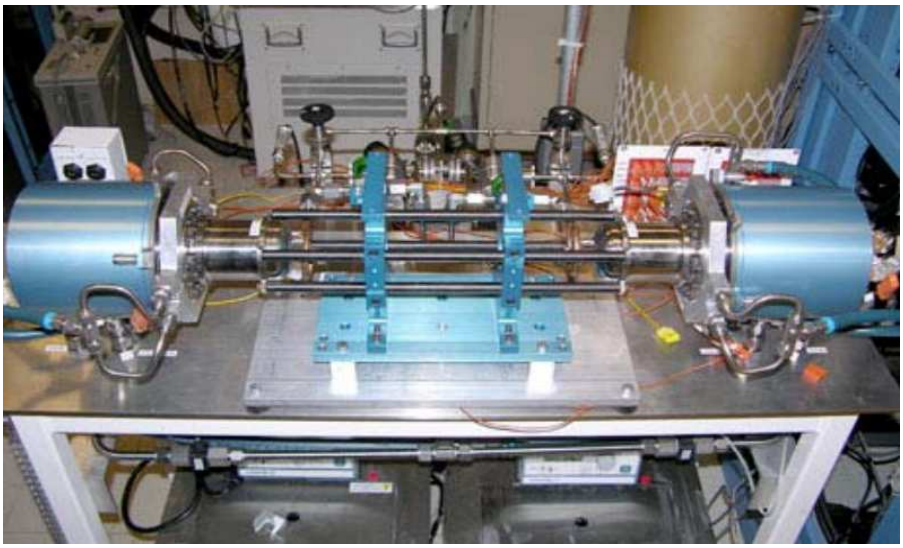

Figure 3: NASA ASC-0 [13]

A few issues that arise with the ASRG and space travel relate mostly to the introduction of moving parts. While an RTG is robust and secure, an ASRG has flywheels and bearings that can be damaged if contaminated with dust or other particles. Additionally, the moving parts introduce vibrations that could cause damage over the course of a mission, which could last up to or beyond 10 years [14]. The startup procedure for a Stirling engine can also introduce issues, as it is often necessary to manually start the engine by rotating the flywheel or compressing the spring. Without the ability to start or restart automatically, the system must include an extra starter or be completely dead once the cycle halts.

Other steady state power production options are less developed but may still have practical uses in the future. One option is an Alpha or Beta Voltaic, which takes advantage of radioisotopic decay ions to create current. As a charged particle is released during decay, it can interact with the electrons of other materials, such as the p-n junctions of a photocell. An alpha particle will remove electrons from one location and deposit them at another as it passes through, thus creating a small voltage between those two points. A beta particle will introduce an extra charge at a certain area, causing electrons to try and flow away from it. With proper material selection and penetration depth calculations of the particles, these electrical forces can be made to create electrical flow. However, the energy imparted into the decay particles is often very large compared to the energy produced by moving the few number of electrons, so by nature the efficiency of these decay batteries is very low, on the order of 4%. [15]

Thermionic technology is another option for long term radioisotope power supplies, theoretically, a hot source could reach such high temperatures that the individual atoms inside it begin to ionize and boil off electrons. Those electrons travel over a small gap and are collected by another material. That material is then negatively charged, and the hot source and collector form an electric potential that can power a circuit [14]. This technology is more

mature than alpha/beta decay batteries, but has some issues as well. First and foremost, the distance the electrons are able to travel is on the order of nanometers [14]. Placing and keeping materials so close can introduce complications, especially when a large surface area is desired and the materials are at high temperatures. Keeping temperatures high enough to cause ionization can also be difficult for a radioisotope, because the power levels are lower than chemical or fission sources in exchange for their lifetimes being much longer.

Radioisotope Thermo-Photovoltaic (RTPV) technology uses a radioisotope heat source, the photons emitted through radiative heat transfer of the source, and a photovoltaic cell to produce electrical power [1]. As the radioisotope decays and gives off heat, its heat transfer pathways are limited by functioning in a vacuum and by having very minimal contact support. This causes the source to reach high temperatures where it can radiate the heat away through photonic emission. Based on what material is radiating and at what temperature, the wavelength of the emitted photons can be "tuned" to the wavelength desired by a photovoltaic (PV) cell. That is to say, the majority of the photons can be emitted within a specific wavelength band, increasing the conversion efficiency of the PV cell. The tuning of a blackbody emitter to a GaInAs photocell is illustrated in Figure 4.

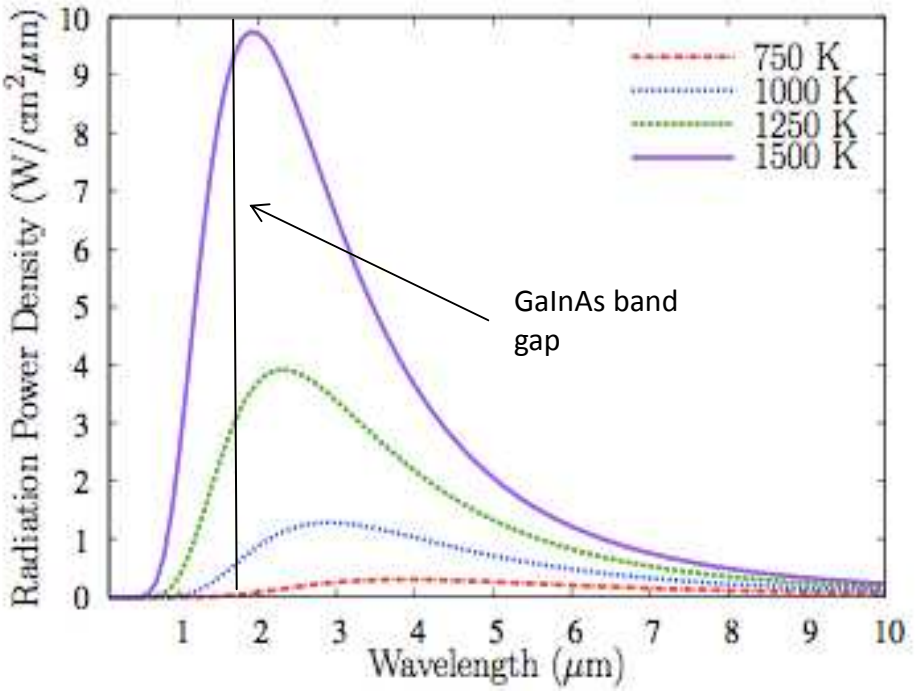

Figure 4: Photonic emission peaks at different temperatures of emitting blackbody [14]

RTPV systems are viable for space travel because the vacuum they use to reduce convective cooling is already present, and the lack of moving parts allows for a very long lifetime. Proper tuning of wavelengths ensures a high conversion efficiency, and the materials used and manufacturing methods of the device are understood and easily used. However, they are slightly more fragile than MMRTG systems due to the PV cells and minimized mounting system. A closer comparison of energy production methods is explored below.

1.1.2 Comparison of Other Options

Given the four major choices above, MMRTGs, decay batteries, thermionics, and RTPVs, a comparison can be made to determine which technology may provide the best option for near-term space exploration. Total efficiency, robustness, radiation effects, and manufacturing feasibility criteria show the strengths and weaknesses of each method in the table below:

Table 1: Comparison of power systems

Radioisotope power source comparison chart					
	MMRTG	ASRG	Decay battery	Thermionics	RTPV
Efficiency:	6%	26-28%	<4%	5-20%	15-30%
Robustness:	Highest	low-moderate	high	low	moderate
Radiation shielding:	moderate	high	low	high	high
kg/kW	350	~200	300-400	200-300	100-200
Manufacturing:	moderate	easy	easy	difficult	easy

The total efficiency for each system shows how much electrical power can be produced per unit of thermal power. The MMRTG has been empirically measured, and decay batteries have been used on small scales, while the other sources rely on separate components being tested and an efficiency hypothesized. Due to this, a wide range of possible efficiencies exists.

The robustness metric is representative of the device's ability to suffer impact or survive long term use. MMRTG's have no moving parts and are relatively stable. ASRG's, however, can be shaken, contaminated, or otherwise break down if damaged. Decay batteries and RTPV systems can be made from strong materials with the exception of the photovoltaic cells, and thermionics are prone to cause contact between the minimally spaced anode and cathode when jolted.

Radiation shielding refers to how much of the decay product is restricted to a safe area. Almost all systems can be encapsulated in sufficient shielding to diminish the majority of harmful particles. However, shielding adds mass to a system, which increases cost drastically. When comparing inherent shielding possibilities, the MMRTG has some amount of housing/cladding, while decay batteries rely on exposed sources to function. ASRG's, thermionics, and RTPV's could use a solid ceramic-metal (CerMet) fuel source to encapsulate the

radioisotope source while still maintaining desired surface features and emissive properties. CerMet radioisotope encapsulation technology is currently being researched by the Center for Space Nuclear Research in Idaho, where PuO_2 ceramic powder is mixed with a tungsten alloy blend. The ceramic and metal powders are then spark plasma sintered under high temperatures and pressures, and introduced to a large electrical current which presses the powder into a single solid unit. The metal matrix provides thermal conductivity to the solid fuel system, while simultaneously providing shielding. This technology could also be used for RTG technology if not for the requirement that they now all use GPHS units [10].

The kg/kW metric is useful in understanding the cost vs. effectiveness of a system, as the driving factor in calculating cost is the total mass. Each unit of mass needs a large amount of fuel during launch to escape gravitational forces, and having a low mass and high electrical production results in a cheaper, more effective system.

Lastly, the manufacturability of each system can be compared based on its solid fuel unit. An MMRTG unit is assembled by pressing PuO_2 into pellets, inserting them into the housing assembly and stacking the fuel bricks together. This exposes any workers to a hazardous amount of radiation if not performed with extreme care. Thermionics have to be placed with such tight tolerances that they require manipulating radioisotope loaded materials for long periods of time into complex geometries. ASRG, thermionics, and RTPV units can be assembled without the fuel present, which can be inserted later. Using spark plasma sintering technology, the radioisotope can be encapsulated in a CerMet at a remote location and easily placed in the device when needed.

From the comparison it can be seen that ASRG, thermionics, and RTPV technologies are capable of providing the highest efficiencies, and likely the highest power to mass ratios. This makes them the obvious front runners for space power production devices. However, only

RTPV has the increased robustness that comes from a static design and simple geometric construction. While it may not be as tough as an RTG system, it can still maintain structural integrity though normal, expected vibrations and impacts.

1.2 Uses for Radioisotope Power Sources

There are many devices which could benefit from a long term power source, on the earth and in space. Large scale RTPV systems could be developed for baseline power for cities and towns, be they remote or in large population areas. The CerMet encapsulation of the radioisotope makes removing any hazardous materials extremely difficult, and they have no risk of meltdown or explosion because they never approach critical levels.

Additionally, areas such as the earth's poles or isolated areas sometimes need equipment to function for years. Feeding power to the installation can prove to be a difficult challenge. Currently, off-grid equipment is moving towards either solar, wind, or diesel power to function [16]. These devices are large and heavy, and provide wildly varying power levels at different times. Providing them with RTPV generators could allow for data to be taken for extended periods of time without any human intervention, local power plants, or power fluctuations.

The field that most uses radioisotope power systems of course is space exploration. Recently, the focus of space exploration has switched from large expensive missions to smaller, less expensive possibilities. From this, the idea of CubeSats arose [17]. CubeSats are small, 10cm x 10cm x10 cm satellites that house small equipment packages for minimal research goals. These satellites can be customized based on the desired mission, and more importantly, are significantly less expensive than most other satellite options. They still require launch vehicles

and rockets to reach their destinations, but once placed can function autonomously. Figure 5 shows an example of a CubeSat design.

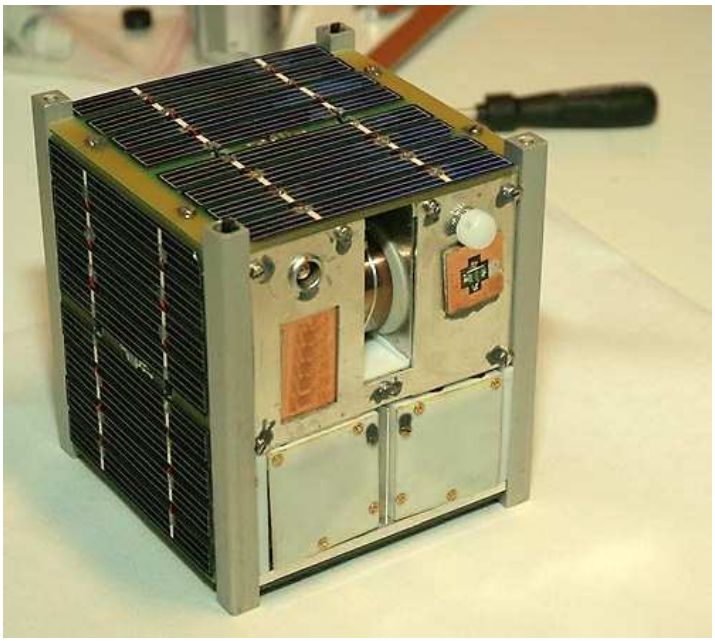

Figure 5: CubeSat [17]

The drawback of the CubeSat design is the lack of power systems. Currently, they can be covered in small photovoltaic panels, but as the distance from the sun increases, the power they produce decreases. Without an appropriately sized power source, CubeSats are not a viable option for exploring the outer solar system. However, due to the CerMet encapsulation technology used by RTPV devices, they can be made to much smaller power levels than RTG systems. An RTPV power source could be custom built to fit the needs of small CubeSat missions, thus enabling the use of these inexpensive satellites in the far reaches of space.

1.2.1 Other RTPV Options

Once the technology for thermo-photovoltaics matures, we may start to find it more commonplace in our everyday lives. The estimated conversion efficiencies are on par with

current energy production methods, and the technology could be adapted to function on a larger scale. Even by using the same fuel (such as coal or natural gas) the conversion method from thermal energy to electrical could replace turbines, cooling towers and large amounts of plant infrastructure. Nuclear plants could change from a Rankine cycle method to a RTPV conversion while still maintaining a critical assembly. With thermo-photovoltaic technology, the power output of a plant could change as quickly as the temperature of the emitting source changes.

Cars, planes, and boats could also save huge amounts of space by replacing their fuel tanks with a radioisotope fuel source and their combustion engines with electric ones. Gearing up the current RTPV designs to produce high enough power would be a clear obstacle, as well as putting radioactive material within the reach of the general population, but it is conceivable that someday thermo-photovoltaic batteries could provide long lasting, clean power to individuals around the world.

1.3 Literature Study of Thermophotovoltaics

TPV devices have been researched since the 1950's but have not met with commercial success due to limitations on materials and temperatures [1]. Kolm, a researcher at MIT was first tasked by a defense department request with generating electricity from a lantern flame, which he achieved by using a silicon solar cell [4]. Work persisted until recently with low conversion efficiencies until new materials and methods could be developed.

Recently, NASA has done the bulk of research at NASA Glenn Research Center in Ohio. [1]. However, NASA prefers their power source to be a NASA developed GPHS unit, which is described in more detail below. This unit requires layers of shielding and structural support, as well as a limited power density. Donald Chubb is considered to be one of the foremost experts

on RTPV design, contributing to many works and publishing a text on the subject [1] [18]. Other private entities, such as Orbital Sciences [19], EDTEK [20], and General Atomics [21] have also been researching RTPV technology over the past few decades. Results were generally positive in regards to RTPV performance, but required very high temperatures and simpler alternatives were often favored.

Currently, MIT is developing highly effective selective emitter technology known as photonic crystals [22] [23]. The technology artificially creates a selective emitter that has very low emissivity values at undesirable wavelengths, and high values at useful wavelengths. The Center for Space Nuclear Research in Idaho has been investigating radioisotope encapsulation through CerMet technologies in order to provide a more effective fuel source and emitter [35]. This CerMet fuel greatly reduces radioactive levels outside of the fuel, provides structural support, and allows for surface features such as selective emitters or photonic crystals to be included as a part of the fuel instead of an additional shell.

Research also continues on the performance of photon conversion technology, specifically in the infrared range for systems which do not take advantage of the large solar spectrum range. NASA Glenn has contributed to the development of Indium-Gallium-Arsenide solar cells to improve RTPV conversion efficiencies [24]. Other entities are also exploring infrared cells for multi junction solar conversion, such as Columbia University and the University of Science and Technology of Hebei, China [25].

With all of these improvements made to RTPV technology over the years, the concept is becoming more viable as a power source for extended life missions. Bringing these aspects together is integral in improving the power generation possibilities of space exploration and adapting them to new and innovative technologies.

Chapter 2: Development of RTPV Power Sources

2.0 Basics of Development

In order to design and build an RTPV system, there are certain factors which must be modeled and understood before construction begins. The major factors to consider include power limitations, power conversion, thermal losses, and emissivity properties of the system.

Each radioisotope has a certain power density as a pure element, that is to say it produces a certain amount of thermal power per kilogram of material. Highly power dense materials decay faster. They have shorter half-lives and often give off more dangerous radioactive particles. The amount of power generated must be large enough to combat the energy losses in order to reach the desired temperature, but not so large that it damages components or passengers.

Converting the thermal energy into electrical is done by reaching high enough temperatures to emit the proper spectrum of light, and then absorb that spectrum with a photovoltaic cell. This can be done by measuring the emission spectrum of different materials and comparing it to the response curves of photovoltaic cells, or by heating a material until it emits the desired spectrum and collecting the light directly with a PV cell.

The emissivity of each component must also be tightly regulated as radiative heat transfer is the primary cause of loss in the system. The lower the emissivity of a surface, the less energy it loses by radiating. Keeping the emissivity as low as possible forms a sort of "optical insulation" where energy cannot escape. High emissivity values for the emitter material may keep the majority of the emitted light in the desired spectrum, but lower the overall temperature of the heat source. When an object is opaque at all wavelengths in question, emissivity, ε, is related to reflectivity, r, for each applicable wavelength by Equation 2.1 [1]:

$$\varepsilon_\lambda = 1 - r_\lambda \qquad [2.1]$$

The heat lost by radiative means is given by the Stefan-Boltzmann Law, Equation 2.2:

$$Q = \varepsilon_\lambda \vartheta A(T^4 - T_0^4) \quad [2.2]$$

Where Q = power (w), ε_λ = emissivity at a specific wavelength, ϑ= Stefan-Boltzmann constant (5.67x10^{-8} W/(m^{2}K^4)), A = surface area (m^2), T= surface temperature (K), and T_0= ambient temperature (K).

Thermal losses can also play a major factor in the heat transfer of the system. The hot fuel source must be suspended away from the photovoltaic cells and structural housing, but still held secure enough to resist vibrations and impacts. The thicker the supports, the easier it is for heat to escape. Conductive heat losses behave as per Fourier's Law, Equation 2.3.

$$Q = kA(T_H - T_L)/L \quad [2.3]$$

Where Q = power, k= thermal conductivity, A= cross sectional area, T_H= hot side temperature, T_L= cold side temperature, and L = the distance across the temperature difference.

As an interesting tradeoff, many conductively insulating materials have high emissivity values, which at high temperatures can cause radiative losses. Ceramics, for example, are often good insulators but are rarely reflective.

Once these aspects are understood, a testing rig can be designed to prove the concepts and measure exact values in question. Then an RTPV system can be designed based on these concepts and values.

This process is explored in more detail below.

2.1 Power limitations

Currently, plutonium oxide, or PuO_2, is used as a radioisotope power source for many space missions, as it is the current fuel used for the GPHS. It uses isotope 238, which has a power density of ~540 W/kg when new. When combined with oxygen to make PuO_2, the power

density drops to around 345 W/kg. When inserted into the tungsten alloy matrix to create the solid fuel emitter of the RTPV system, the power density drops again, to approximately 160 W/kg. All these steps are necessary, however, to prevent the metal plutonium from melting at low temperatures, and to provide adequate shielding and structural support to the fuel.

Power density is an incredibly important aspect of RTPV systems because the temperature of the system is directly related to the power generated vs. the power lost. In this case emissive losses can be a huge part of those total losses. The surface area of the emitter is the source of those emissions. Therefore, having high power and low surface area is a necessity. Different radioisotopes have different power generation capabilities and are discussed in detail in Section 2.1.1.

At least three options are available to simulate the heating effects of plutonium on the CerMet core. The simplest option is to use a small microheater to impart energy into a material sample. This option is capable of raising the temperature of the material to the same temperatures found in an RTPV system, but does not account for total power in to the system, radiative or conductive losses from the heater to the sample, and may introduce light pollution when measuring emitted spectra.

A second option is to heat a CerMet sample though RF means, essentially microwaving it until it reaches temperature. This method, however, will also heat any mounting system as well as any instruments inside the heating volume, such as thermocouples or fiberoptics.

A third option is to use laser heating. In this method, a laser beam targets a small sample of material and brings it up to temperature. The problem with this method is the emissivity, and thus reflectivity, of the sample changes with temperature. Consequently, it is difficult to tell how much power is being deposited into the sample. To combat this, a blackbody cavity can be inserted in to the sample as a laser target. That area will always have an

absorptivity and emissivity of one, which allows for accurate calculations. Additionally, the beam is fully absorbed and there is no danger of light pollution or instrument damage from the power source.

2.1.1 Other isotopes

To more clearly understand the tradeoffs between isotopes that can be used a chart of nuclides can be used to determine decay chains and radiation tendencies [26]. By doing so, it can be concluded that the front runners for RTPV power are plutonium, americium, curium, and strontium. Strontium seems like a good candidate due to the controllable decay products and high power density, but along the decay chain one of the daughter elements emits a mega-eV gamma ray which is incredibly hard to shield against. Curium also has a high power density, but the neutron flux it produces is so large that for an RTPV system, the exposed photovoltaic cells would suffer massive damage. Americium is easy to shield against, but has a low power density, which in the case of RTPV systems means it would have to be very large to achieve proper volume to surface area ratios. When the shielding of a system is included, the benefits of a very power dense radioisotope can be lost due to the addition of large or heavy shields. Because of these reasons, plutonium was deemed the best radioisotope fuel source, although under certain circumstances the others may yet find themselves to be viable alternatives.

Other at-risk components for radiation damage include electrical components or living passengers. For current missions, the RTG power sources are attached to an extended boom which keeps the source far enough away from sensitive parts to remain safe. However, some isotopes can still be dangerous at that distance without proper shielding. It is a goal for RTPV power sources to be able to be housed inside or near the scientific payload in order to reduce boom mass and overall system volume by using proper shielding.

Table 2: Comparison of radioisotope power sources

Element	Power Density (W/kg)	Half Life (Years)	Benefits	Issues
Am241	90	432.7	low amount of hazardous radiation	low power density
Pu238	500	87.7	good balance of power density and low radiation	limited supply
Cm243	2500	29.1	very high power density	very high neutron flux generated
Sr90	931	28.8	high power density	daughter (Y-90) emits >2 MeV gamma

2.2 Thermal to electric conversion

The conversion of thermal energy to electrical energy goes through three phases: thermal, radiative, and electrical. First, the thermal energy is produced by the decay of the radioisotope source and the collision of the decay fragments with the surrounding material. As the system heats up, it converts the kinetic energy of the individual atoms into photonic energy at the surface, emitted as thermal radiation. There is no inherent loss of energy between these two energy types. However, controlling the energy flow can prove difficult, and thermal and emissive losses will reduce the overall efficiency of the system.

When the emitted photon reaches its desired target, the photovoltaic cell, it participates in the photovoltaic effect to produce electrical power. The photovoltaic effect is a phenomenon wherein the wavelength of a photon is the right size to excite a valence electron of some material through the “band gap” of the conduction band. That material is contained in a positive-negative, or p-n, junction which creates a small push on every electron in the material. Once an electron is excited to the conduction band, it is easier to move and it begins to flow towards the positive side, thus creating current. Conversely, the “hole” created by the moved

electron moves in the opposite direction, shifting neighboring electrons down and resetting the system.

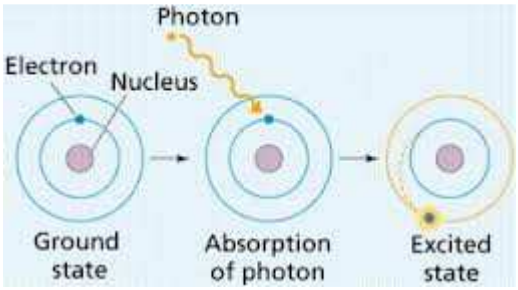

Figure 6: Electron excitation by photon [27]

The conversion of light to electricity is dependent on two efficiencies: quantum and conversion. The quantum efficiency of the system refers to how many photons successfully interact and excite electrons in the material. If every photon incident on the PV cell creates an electron-hole pair, it has 100% quantum efficiency. If there is a range of wavelengths incident on the material, some of the weaker photons will not have the energy to excite the electron, and may drop the quantum efficiency. Additionally, a large amount of photons on a small area will not allow the system to reset between electron-hole pair creation, and the quantum efficiency will again decrease.

The conversion efficiency factor takes into account total electrical power produced by the photovoltaic cell vs. total photonic power incident on the cell. This is largely due to wasted energy by the photons and the nature of the p-n junction. If a very high energy photon interacts with the atoms of a photovoltaic cell, it may have much more than the required energy to create an electron-hole pair. In this case, the excess energy is deposited as thermal energy. Even if a cell has 100% quantum efficiencies at 0.5eV and 1eV photon energies, the electrical production will be the same, and 0.5eV per photon will be wasted per 1eV photon absorbed.

The nature of the p-n junction is also important, because the flowing electron-hole pairs will not necessarily have the same electrical energy output as the energy level of the photon that caused it. Once the electron has been excited, all the energy of the photon has been absorbed and it is up to the p-n junction to push the electron. Generally speaking, a higher energy band gap means a higher power photocell. [28]

In order to minimize losses during power conversion, the thermal and emissive losses must be minimized by adding thermal or optical insulation wherever possible. The quantum efficiency must be maximized by tuning the emitted wavelength to the desired wavelength of the photovoltaic cell. In addition, the conversion efficiency must be maximized, usually by increasing the paired wavelengths as high as possible to ensure good p-n junction performance.

2.3 Thermal losses

Minimizing thermal losses is one of the primary goals of the experimental setup, because temperatures can be measured at a variety of points in order to verify experimental results with theoretical calculations. The heat transfer properties of many materials are documented and recorded. Consequently, comparing thermal losses to modeled losses should be relatively accurate. At that point, any variation between experimental and computational results can be attributed to emissive losses, which are much more complicated.

Isolating the heat source introduces some interesting and complicated issues, the most prevalent being the structural support vs. heat loss relationship. As the cross sectional area of a support unit increases, so does its overall thermal conductivity. This has lead to discussions regarding metallic vs. ceramic supports, stands vs. cables held in tension, or spring shaped supports. The experimental process described in this thesis evaluated many of these options, and minimizing losses through the legs became a very large part of the experiment. Even so,

there is no way to completely eliminate the flow of energy through the mounting system and in to the housing.

The hazard involved with this scenario revolves around the temperature limitations of the photovoltaic cells. Most cells lose efficiency as their temperature increases, to a point where they are only usable below 85 °C (358 K) [29]. If this were not the case, the housing could be allowed to increase in temperature and hinder the flow of energy out of the emitter surface. But because that is not the case, wasted heat must be actively rejected before it reaches the photovoltaic cells, and the emitter will cool rapidly if given the opportunity.

2.4 Emissivity

Radiative heat transfer occurs on the surface of materials as the kinetic energy of moving atoms forces electrons to move, and the resulting movement creates a photon which removes energy from the system. This usually takes place in the range of 0.1 to 100 μm, a range which is known as the thermal radiation heat transfer band. The willingness of a material to emit these photons is referred to as emissivity. Objects that are very reflective have very low emissivity values, and objects that are very matte usually have very high emissivities. Emissivity values can range from 0-1, and it is related to a number of different other optical surface features. As seen from Equation 2.1, emissivity and reflectivity must add up to 1 for an opaque object. Additionally, when an object is exposed to incident light, it must either reflect, transmit, or absorb that light, which gives rise to Equation 2.4 [1].

$$r_\lambda + t_\lambda + a_\lambda = 1 \qquad [2.4]$$

Where *r* is reflectivity, *t* is transmissivity, and *a* is absorptivity, each at a specific wavelength.

If the object is opaque and has no chance to transmit the light, the equation can be reduced to:

[2.5]

Substituting in Equation 2.1 for *r*, it can be seen that absorptivity is equal to emissivity. This is known as Kirchhoff's Law. The tendency of an object to absorb light from the outside environment at a specific wavelength is just the same as its tendency to emit light back into that environment at the same wavelength. This can create issues when an object is absorbing a different wavelength of light than it is emitting, but in general an object that absorbs light easily will also emit easily. The exception to this rule being selective emitters, as discussed below.

An object with an emissivity value of one across all wavelengths is referred to a blackbody emitter. A blackbody emitter has a specific emission profile of radiance (or intensity) vs. wavelength, which changes at different temperatures as seen in Figure 7.

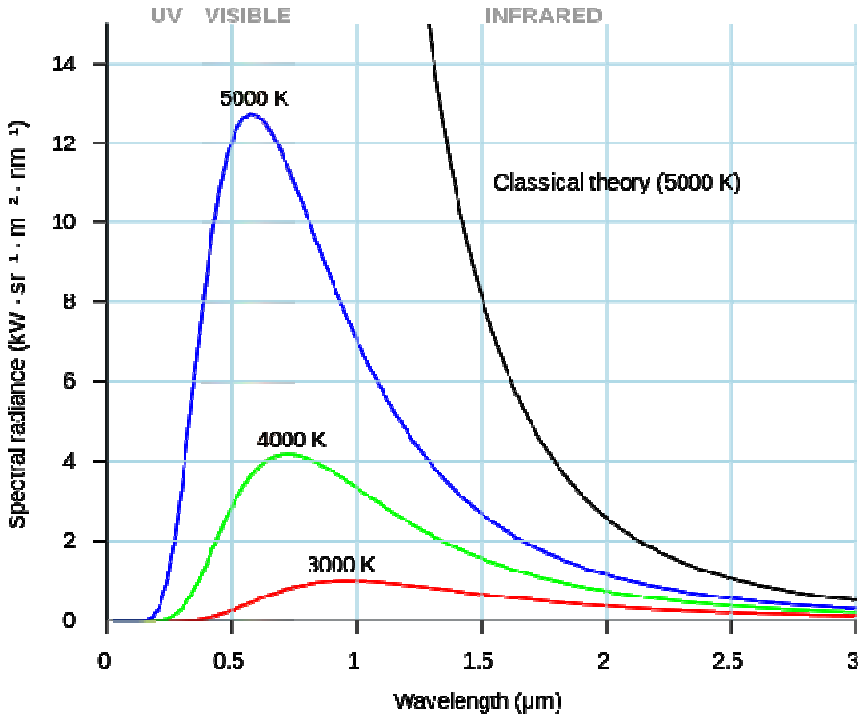

Figure 7: Blackbody curves at different temperatures [23]

The profile of a blackbody is given by Planck's Law (Equation 2.6).

$$B(T) = \frac{2hc^2}{\lambda^5(e^{\frac{hc}{\lambda T k_B}} - 1)} \quad [2.6]$$

Where B is the intensity, T is temperature, h is Planck's constant, λ is wavelength, c is the speed of light in the medium, and k_B is the Boltzmann constant.

Objects that have similar emission profiles are referred to as "gray bodies," because they may behave similarly to black bodies but do not have perfect emissivity values of one. Gray body emissions will be slightly smaller than blackbody emissions, or have certain imperfections at specific wavelengths depending on their properties. Other emitters are referred to as "selective emitters" which have certain emissivity values at different wavelengths. A selective emitter may have a certain total emissivity value, but different emissivity values at different wavelengths. Some common selective emitters are ytterbium, erbium, and cesium [1]. These selective emitters allow for preferential absorption or emission based on the wavelengths where they have high emissivities.

Selective emitters are of particular concern for the development of RTPV's because they can help to emit the desired wavelength of light for the photovoltaic cell while keeping total emissivity as low as possible in order to raise the temperature of the system. A perfect selective emitter will have defined emissivity values at each wavelength or range of wavelengths. Figure 8 shows an ideal selective emitter with emissivity of one for all wavelengths below 2 μm, 0 for all above. It is compared to a variety of real world selective emitters which do not have the perfect, distinct edges of the ideal case.

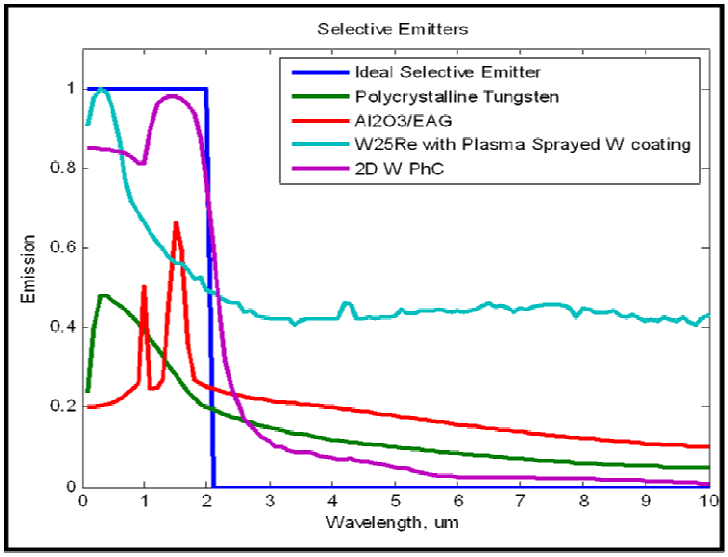

Figure 8: Emissivities of some selective emitters [23]

Even though selective emitters have responses that are tailored to specific wavelengths, they still must be "tuned" by adjusting the temperature to achieve the maximum output within the desired range. This is because the actual emission spectrum is different than the emissivity spectrum shown above, because it must be multiplied by the blackbody curve of the surface at the given temperature to give total radiative intensity. For the perfect selective emitter shown in Figure 8, a sample at low temperature would have no emission at 2 m, and even though the emissivity at 2 m was one, or 100%, no light would be emitted at that wavelength. Looking back at Figure 4, it can be seen that a sample at 5,000K has a peak well beyond the 2 m, and the selective emitter would only cut off the tail. Setting the emitting surface to the temperature that naturally emits the majority of power at the desired wavelength ensures that the most efficient light escapes, while the less useful light is prevented from being emitted.

New materials that may assist in the tuning of the emission spectrum are called photonic crystals, and are under development at MIT [22] [23]. Photonic crystals are primarily used to limit the passage of electromagnetic waves through material by creating a repeating pattern of dissimilar materials in a grid shape. When EM waves attempt to enter the structure,

there is no solution to the waveform equation inside and the light cannot exist. A row of structures is then slightly changed to allow the existence of a certain wavelength of light, and the light can follow the chain of changed objects with 100% transmission, essentially creating a very efficient fiber optic. However, when created as an emitter material, the repeating pattern can instead be used to emit light of that specific wavelength, allowing for only one wavelength to exist. By doing so, photonic crystals can theoretically create a perfect selective emitter that gives of the specific wavelength required by the design.

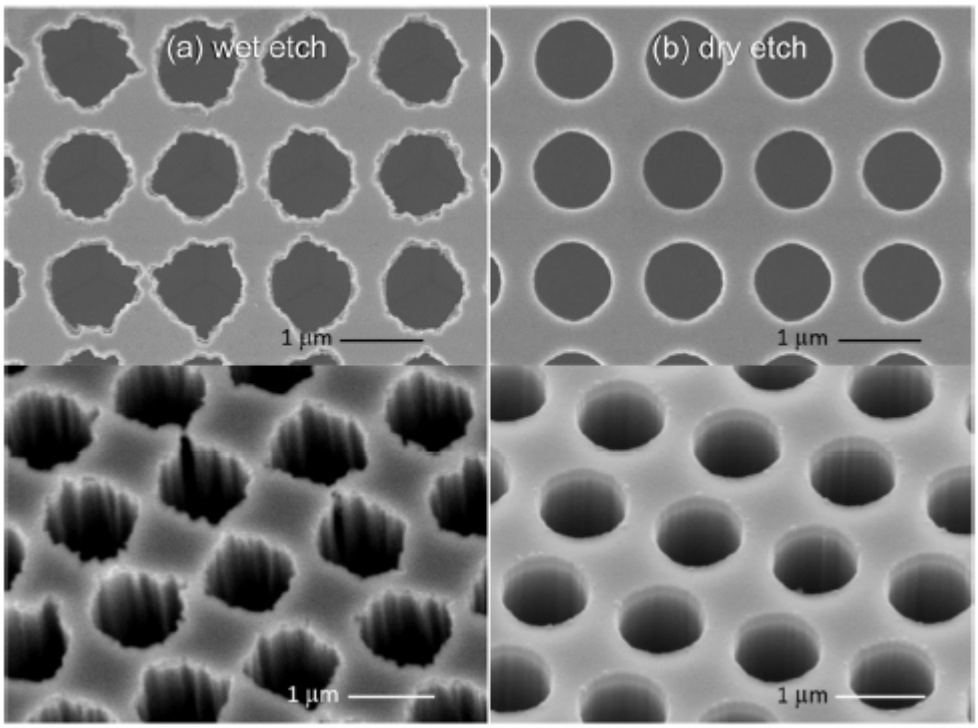

Figure 9: Photonic crystals used as emitters [23]

The peak of the blackbody curve can be estimated by Wien's Displacement Law (Equation 2.7).

$$\lambda_{peak} T = b \qquad [2.7]$$

Where λ is wavelength (μm), T is temperature, and b is a constant which has a value of 2.8978x10^4 μm *K. By solving for the cutoff wavelength of 2 μm, it can be seen that the tuning

the peak emissivity to the cutoff wavelength would take a temperature of ~1,448.9 K. Depending on the response curve of the photovoltaic cell that desires to convert these photons, the temperature could be increases to a value past this number to ensure maximum conversion from the useful spectra of light.

2.5 Test Setup Concept

In order to create an experimental testing setup capable of simulating the heat generation, heat losses, and emissivity properties of a functioning RTPV system, many factors were taken into account and the following configuration was settled upon as a starting point.

In order to generate the necessary heat in the proper location, laser heating was used. The laser heating method was found preferable because the power output could be easily traced from the laser controller, it has a small, specific area of heating, and it would not heat or damage other components in the design. The variable power level is also useful to match different solid fuel configurations, as a plutonium based source would have very different dimensions than a curium based one. With the variable laser input, a variety of different sizes and radioisotopes can be simulated.

The laser target used to simulate the radioisotope loaded CerMet fuel was a small cylinder the dimensions of the fuel source formed into a blackbody cavity. A blackbody cavity is a design wherein a large cavity has a single small hole in it to allow for the transmission of light. That aperture will allow light to enter, but not exit as the beam reflects inside the cavity until total absorption is achieved. Additionally, it emits light as a perfect blackbody, but only in the area covered by the aperture. In this case, that meant that the laser beam could be 100% absorbed as it entered the blackbody cavity, and the large emissivity value of the perfect absorber/emitter was limited to the area of a small hole.

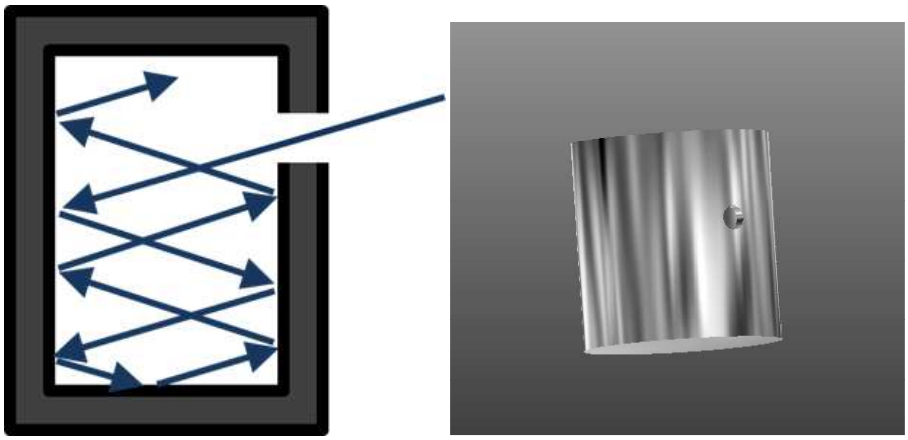

Figure 10: Blackbody cavity illustration [30] and artist concept

In order to ensure the entire beam was absorbed by the target, a small lens could be used to focus the beam inside the cavity.

The cavity could be made of whatever material was of interest for the solid fuel. If a wide variety of samples was intended to be tested, the can may be constructed of a low emissivity material and the samples tested individually. Samples of material could be placed on top of the target and heated conductively to high temperatures. These samples would allow the testing of selective emitters without the need to coat the entire surface of the target before each test. Although this method would allow for more rapid testing, it would also introduce a contact loss between the target and the sample.

Enclosing the entire system in a vacuum would simulate the vacuum of space as well as remove any convective losses to the system. Vacuum chambers can be made of a variety of materials, some of which are capable of allowing the laser to pass through to the target. Originally, the enclosure was thought to be made of glass or plastic, but after considering the transmissive properties of the materials it was later changed to steel.

The simplest mounting system devised at the design stage of the experiment was a small stand sitting on four legs with an insulating brick inserted between the target and the

stand. This would simply hold the target in position while the insulation limited the flow of energy through the legs.

A spectrometer would be attached to the system by means of fiberoptic cable to record the emission of light from the test sample.

Lastly, thermocouples would be attached at different points during different experiments to help understand the heat loss mechanisms. Points of interest include the laser target, sample surface temperature, and mounting leg temperature.

COMSOL (CAD) models were used to verify all findings in order to ensure accurate data that could then be used to adapt the material and system properties into a theoretical design for an RTPV system. Figure 11 shows the initial concept of a laser heating a target which emits to a spectrometer above.

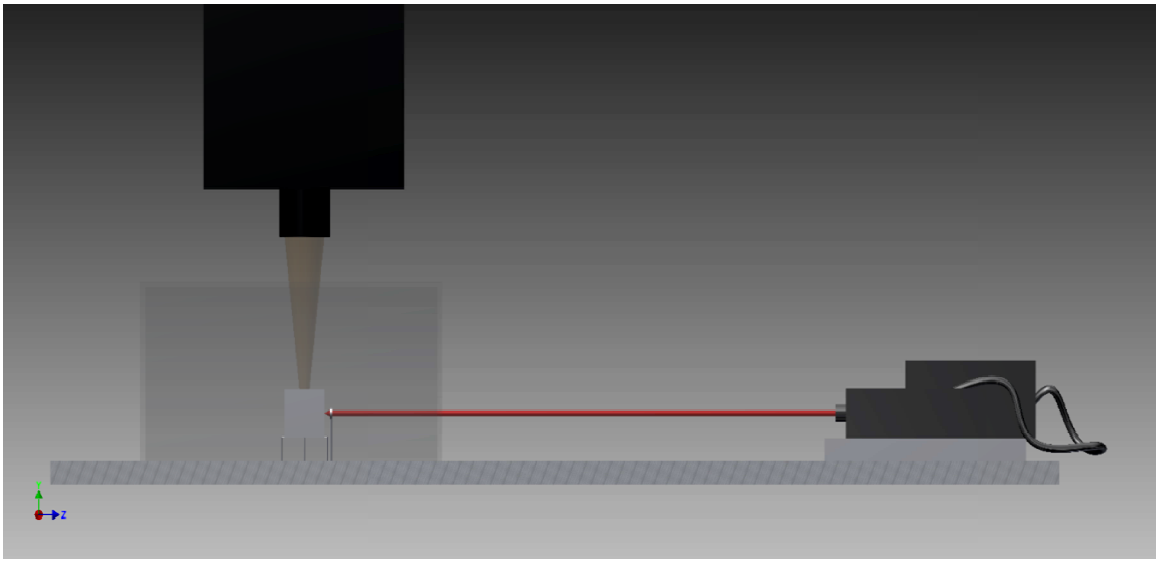

Figure 11: Initial concept of experimental setup

Chapter 3: Experiment Design

3.0 Experiment Design Overview

The purpose of this experimental setup was to gather empirical data about the material properties and viable configurations used in RTPV design for the purpose of adapting computational models to real-world situations. This took place by designing a testing system and changing it after each test to pin down values and determine optimal configurations. For the purposes of categorizing the tests, a numbering system is used to classify minor and major changes to the system (1.0, 1.1, 2.0 etc).

3.1 Preliminary Design (Version 1.0)

Preliminary designs were based around an assumed temperature requirement of 1,500K to acquire the sufficient temperature range needed to tune the blackbody emission spectrum to a variety of photovoltaic cells. Initial calculations assuming no thermal losses estimated the laser power necessary at 10 watts, with a total emissivity value of 0.01 over all wavelengths and directions. For the purposes of comparison, polished gold has a total hemispherical emissivity of 0.01-0.06, silver of 0.02-0.08, and nickel of 0.09-0.17 [8]. The 0.01 value was considered to be the best-case scenario achievable with proper manufacturing methods.

An available 10W argon-ion laser was deemed acceptable for the power source based on these preliminary calculations. Because it was readily available in the lab and did not need to be purchased, it was procured. However, further analysis of conductive losses and emissivity values later deemed that power level too low, and the laser was not used.

The target was manufactured by hollowing out a tantalum cylinder, leaving one end and the sides intact. A lid was fashioned to enclose the other end, and a small, 3mm hole was drilled

in the curved side for the blackbody aperture. The total height of the target was 2.54cm, with a 2.54cm diameter and .254cm wall thickness.

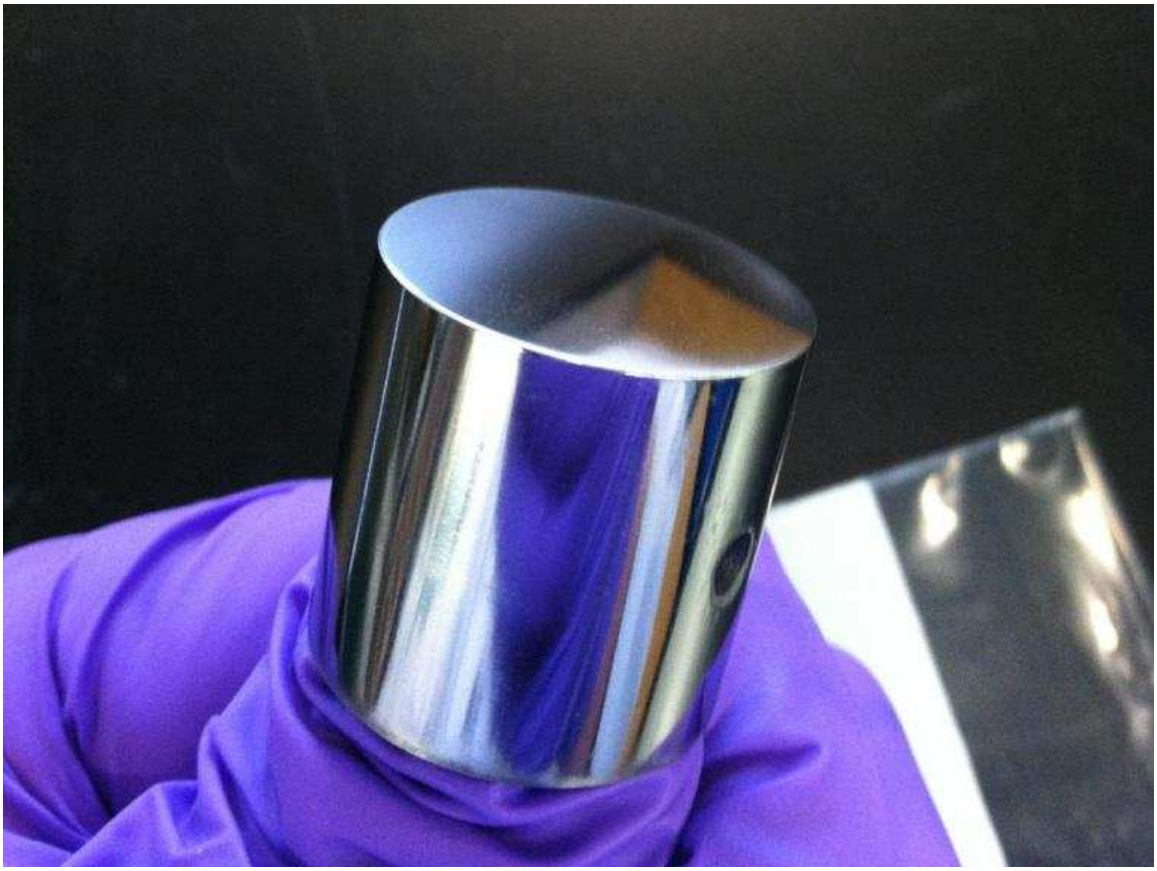

Figure 12: Tantalum can polished to maximize reflectivity

Tantalum was used instead of the tungsten alloy matrix because it is much more malleable and less brittle. Emissivity values are comparable, but due to the need of repeated testing the tantalum was determined to be more durable, and thus a better testing material.

When initially modeling the expected thermal losses through the mounting system, an interesting tradeoff was revealed. Using Microtherm insulation, the thermal resistivity properties seemed to provide excellent insulation, but because the emissivity of the substance was so high, as the hot end rose to the temperature of the target it began to thermally radiate huge amounts of energy, cooling the system. It was quickly concluded that available thermal

insulation would need to stay at cool temperatures itself to avoid hemorrhaging energy as temperatures increases to levels where radiative heat transfer dominated. Because of this, the insulation was placed beneath the legs of the mounting system to allow the thin legs to reduce the heat flow through the legs before contacting the highly emissive surface. Additionally, the small cross sectional area of the legs would leave less of a hot surface exposed on the insulation to radiate.

3.1.1 Location and Safety

Designing an experiment which contains high temperature levels, optical measurements, and laser power systems provided a variety of obstacles to overcome. First, the amount of light pollution must be minimized. Laboratory space with private areas and controllable light sources was necessary. Additionally, the use of the laser required that there be blockades in place to reduce the chances of stray beams hitting unaware targets. Automatic shutoffs needed to be in place to make sure that if any doors were opened the power to the laser was cut off for safety reasons. The laser also required a water cooling system capable of providing 3.8 liters per minute of flow at temperatures remaining under 294 K. Laser goggles, lab coats, and other personal protective equipment was required to keep the users safe from stray laser beams and/or hot surfaces.

With all these considerations in mind, the Radiation Laboratory at the Center for Advanced Energy Studies (CAES) building in Idaho Falls, ID was deemed a suitable location for the experimental setup.

3.2 Immediate Changes to Design (Version 2.0)

After including the expected thermal losses for the experiment, it was concluded that the 10 W argon laser would be incapable of providing enough power to heat the target to necessary temperatures. Instead, at least 30 W would be necessary. Given the tendency for the power needs to increase, it was determined that a laser of even higher power may be needed. This drove the acquisition of a Synrad Firestar Ti-100, a 100 Watt CO_2 laser with a maximum power output of 135 W. The CO2 laser fires an infrared beam, which has a higher penetration depth than optical lasers. The IR beam allowed the target to absorb the heat instead of ablating the surface of the material at high power levels.

CO_2 lasers, however, are not capable of passing through Plexiglas walls of a vacuum chamber. It was decided that a steel chamber with appropriate windows and feedthroughs was preferred. The CO_2 laser emits a beam at 10.6 μm, a wavelength at which zinc selinide (ZnSe) has a >98% transmission [31]. This material was inserted as a window onto the chamber for the laser to pass through. The steel chamber would also be capable of withstanding high temperatures in the unlikely event that the target fell off the mounting system. Given the effective matching of ZnSe to the CO2 beam, it could also be used as the material for the focusing lens. Manufacturer specifications of the ZnSe transmission capabilities are plotted in Figure 13.

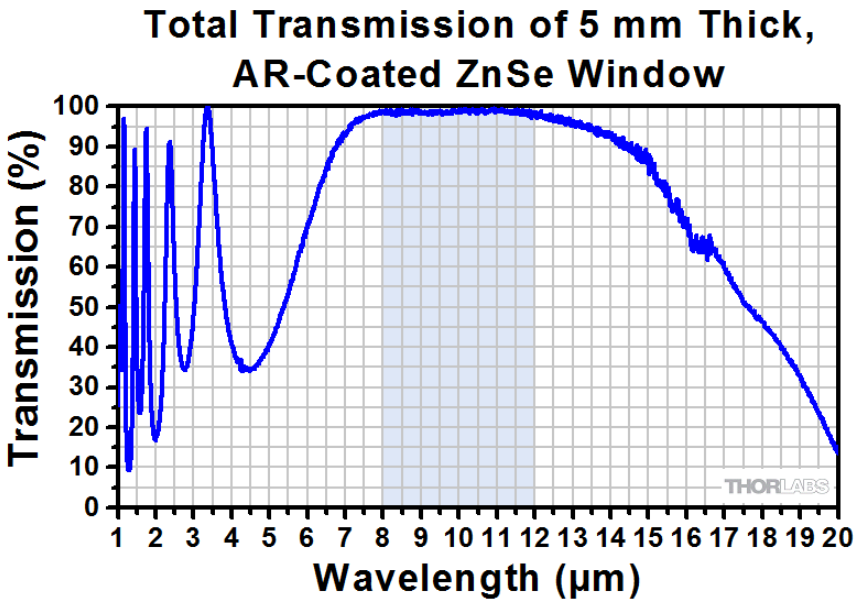

Figure 13: Transmission curve of ZnSe window [31]

Figure 14: Legs at different polishing levels, most polished (left) to least polished (right)

Due to manufacturing and material limitations of tantalum stock, it was decided that the mounting method should change from a detached wire-frame mounting system to a trio of legs welded directly on to the bottom of the target. This would save material. Because the thinnest diameter of tantalum rod available was 0.318cm it was determined that a wire mount would have too much surface area and heat loss. The legs were cut to a 5.08cm length and polished to reduce emissivity. The ends not being welded were sharpened to points to provide minimum contact areas for heat to flow. A picture of the legs at different polishing levels can be seen in Figure 14.

A small bottle of argon was also added to the design to help purge the chamber of any oxygen. The purge would be run before testing for three sets of 10 seconds each to remove air from the system. The argon bottle would then be sealed. After the testing, the inert argon could be used to help the sample return to cool temperatures faster by introducing a convective heat transfer factor.

3.2.1 Changes to Location

Setting up the laser components in a new laboratory introduced unforeseen aspects which were not before taken into account, mainly the lack of proper power supply and time delays in barrier construction. The construction of the facility was unlikely to be completed in conjunction with the proposed deadlines, and the experiment was forced to move into Idaho National Laboratory buildings. Having already hosted laser experiments, the laboratory was more prepared to handle the safety and power needs of the experiment. A diagram of the INL setup from the Laboratory Instruction manual can be seen in Figure 15.

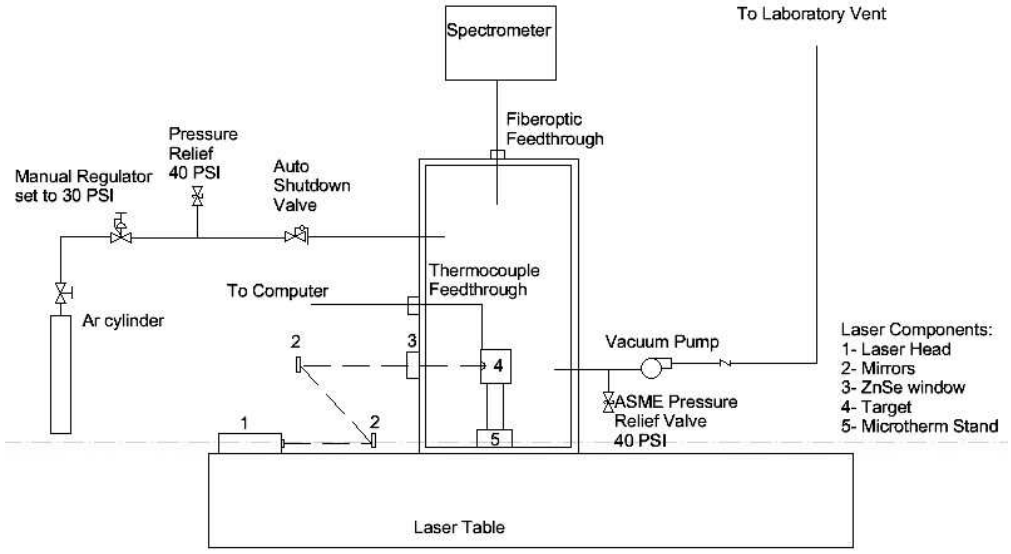

Figure 15: INL Laboratory Instruction diagram

3.2.2 Testing conditions

Inside the vacuum chamber, certain aspects were recorded to ensure the accuracy of the testing. Thermocouples were attached to the back of the target where the beam interacted with the target, and to the lid where the emissive sample would rest. K-type thermocouples were used initially and their errors were measured by measuring the temperatures of ice water and ambient air in the laboratory. The current laboratory temperature was recorded by previously calibrated instruments and read on a digital display. The thermocouples were found to be accurate to $\pm$ 1 K.

The atmosphere in the chamber was pumped down to 400 mTorr in order to simulate a vacuum, but due to a number of feedthroughs and ports on the chamber, as well as vacuum pump limitations a true vacuum could not be achieved. It was decided that because 400 mTorr

was less than 0.1% of standard atmospheric pressure, it would be sufficient to reduce convective heat transfer down to negligible levels. Because the focus of the heating was to reach the desired temperatures, the emissive material sample was not present.

Thermocouples were also attached to the ZnSe window to ensure it was not taking damage from the laser beam, the water coolant input, and the external surface of the chamber to monitor possible stray beams. Once the experiment was fully set up, it was ready for testing. Figure 16 shows the completed setup of the experiment.

Figure 16: Target assembly before first test

3.2.3 Testing Version 2.0

The first test was done by introducing a beam at 10% power (13 W) for a time of 45 minutes. The target rose in temperature to a maximum of 400.85 K at the beam contact point before reaching a plateau.

Next, the power level was increased to 50% (67.5 W) and allowed to heat for an additional several minutes. During heating, the temperature levels suddenly dropped and the experiment was shut down. Upon further review, the anti-reflective coating of the focusing lens had taken critical damage and rendered the lens unusable. The damaged lens can be seen in Figure 17.

Figure 17: Focusing lens damaged by laser

3.2.4 Version 2.1

Given the results of the initial tests, some changes had to be done to ensure the system was working as intended. With the removal of the focusing lens, the aperture of the blackbody

cavity was increased to accommodate the increased width of the beam. Figure 18 shows the diameter of the beam attempting to enter the aperture of the blackbody cavity without a lens.

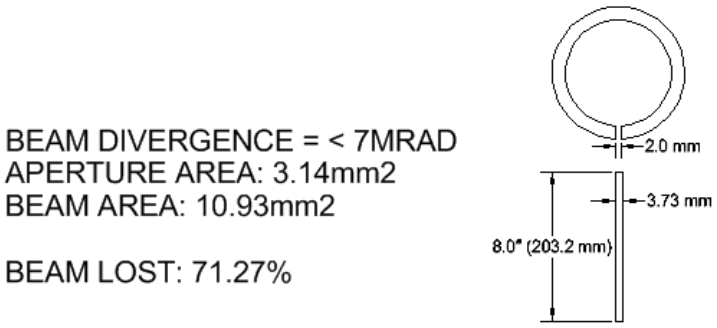

Figure 18: Illustration of beam entering target

The aperture diameter was increased to 4 mm to more closely match the diameter of the beam. Because the aperture hole was not larger, a divot was also added to the back of the target to ensure proper beam diffusion once inside to prevent the beam from reflecting back out.

3.2.5 Testing Version 2.1

Again, the sample was prepared and tested at 10% power for a time of 30 minutes. This time, the maximum temperature at the beam impact point was 446.15 K. The power was increased to 50% and the maximum temperature achieved was 735.15 K at the impact point, while the sample area reached only 714.15 K. Both temperatures were well short of the target of ~1,500 K.

COMSOL models reported an expected temperature of 862K. This number was significantly higher than the recorded values, and thus original assumptions were re-thought. A

new emissivity value of 0.05 was used, under the argument that it was acceptably reflective but there were materials recorded with lower numbers. Therefore, the assumed value was within a realistic range. After testing, it was noticed that a faint, chalky film had been deposited on the sides of the tantalum target and it needed to be re-polished. From this it could be concluded that the emissivity may not only have been higher than previously thought, but the surface of the target could increase in emissivity value as the test progressed.

3.3 Variations in Configuration (Version 3.0)

The mounting system was re-worked in order to reduce losses. The legs were removed to determine a simple case scenario where the target sat directly on the insulation. The results showed that the legs were indeed causing a large amount of loss themselves, and the temperature could vary drastically with different mounting systems. Consequently, a wide variety of mounting systems were used to determine the optimal configuration.

The testing target was periodically re-polished to compare the effects of surface damage. Polishing included multiple steps of silicon carbide grinding paper, working its way down in size from 600, to 800, and finally to 1,200 grit. This provided a mirror-like finish on the surface which would provide the lowest emissivity values available.

3.3.1 Version 3.1-3.9

Determining what configuration would provide the best temperature values in an experimental setting, many tests would need to be performed to determine which tradeoffs produced the best results. First, a test was performed with no legs attached in order to help pin down the emissivity value of the target during testing. Surprisingly, the maximum temperatures increased drastically at 50% power. The impact zone reached a maximum temperature of

975.35 K, while the sample area reached 825.85 K. Figure 19 shows the temperature vs. time history of the heating, with temperature units reported in Celsius.

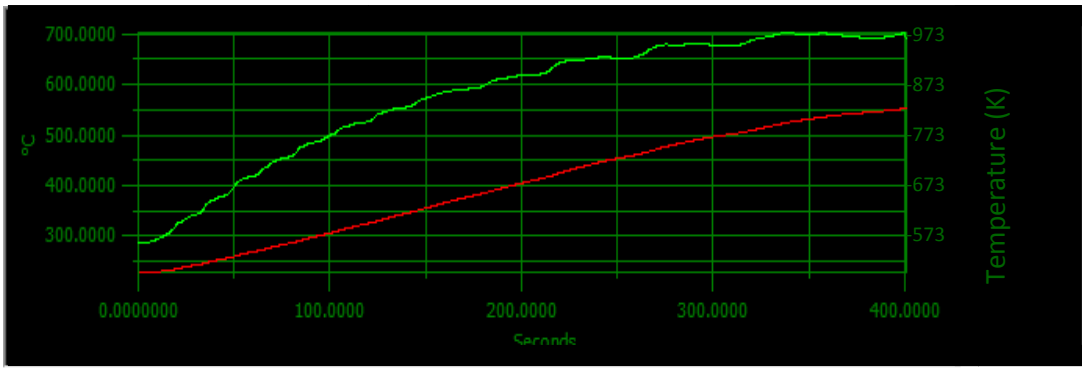

Figure 19: Results of test with no legs, green line indicates impact zone, red indicates top of target

With an emissivity value of 0.2, and the simplified design, the COMSOL model began to match the experimental results at 50% power levels. Additionally, the legs appeared to contribute to the thermal losses instead of hinder them. Sadly, the contact of the target with the insulation at high temperatures resulted in extreme oxidation of the contact points, and there was no way to progress with the Microtherm insulation in direct contact with the target.

A myriad of tests were then performed with different combinations of mounting systems and insulation. Legs were shortened to 2.54cm, small tantalum rods were laid sideways and used as rails, legs were bundled together by tungsten wires and sharpened to points to provide minimum contact, and insulation was switched between Microtherm and Zirconia. Tests were conducted with power levels up to 100 W and the results compared to COMSOL models throughout.

3.3.2 Testing Version 3.1-3.9

Tests were met with varying success, but the maximum achievable temperature was not increasing quickly, if at all. Once performing tests at 100 W, it became apparent that not only

did the laser create a temperature buildup at the impact point, but the laser power itself at those levels was somewhat unstable. Recorded temperatures would fluctuate wildly at that spot, while points away from the area would rise with smooth curves. Cutting laser power would almost immediately cause the impact area thermocouples to read similar temperatures to the other on the target. Because of this, the temperature readings from the impact zone were deemed unusable and eventually not recorded. Previous maximum temperature readings from the impact zones were not considered viable as high temperature records, and were discarded, leaving the maximum temperature thus far at 825 K.

When varying leg length from 5.04cm to 2.54cm, the change had little to no effect on the overall maximum temperature. When reducing the size lower than 2.54cm, such as on short rails, the out gassing of the porous insulation caused the target to oxidize at a much greater rate due to close proximity. Switching insulation types reduced the overall pressure of the system and greatly reduced the oxidation levels. With the more dense insulation, the shorter legs allowed for small contact areas and small emissive areas without taking damage from the gas emitted by the heating insulation. The most effective mounting system, however, was a set of three legs sharpened on both ends and secured to each other halfway down the length. The legs crossed each other to form an hourglass shape. The top of the stand connected with the target on three sharpened points, and the bottom rested on Zirconia insulation on three sharpened points. The maximum temperature on the testing area reached 943 K. The biggest changes to temperature were found immediately after re-polishing the target to ensure a mirror finish, and changing the insulation from Microtherm to a Zirconia disc. This suggests that the emissive value of the radiating surfaces contribute the most to achieving high temperatures.

3.4 Troubleshooting

Even though the maximum temperature was slowly rising with the modifications, the COMSOL modeling was still predicting much higher temperatures at high power. Oddly, the model remained fairly accurate at predicting temperatures at lower laser powers. The values of conductive heat transfer properties provided by COMSOL defaults were validated by independent sources and found to be reliable. It appeared that the error must stem from the emissivity values of the components.

The creation of an oxide layer on the target would no doubt increase the emissivity of the material, but with the removal of Microtherm and addition of Zirconia insulation, the oxidation had decreased dramatically. Further investigation of the subject revealed that not only was did the emissivity profile change with temperature, but the very emissivity values of materials could change as well. Tungsten, for example, varied from reported emissivities of 0.02 at room temperature to 0.28 at 2,273 K [31]. With the addition of an oxidized layer, the values could be significantly higher. To effectively model this phenomenon, an equation of emissivity was added to the COMSOL calculations to predict the emissivity of the tungsten surface based on empirical data. With the inclusion of this aspect, the model became much more exact and became a useful tool for performance prediction. An example of the experimental model (Figure 20) and the computational model (Figure 21) can be seen below for the same test.

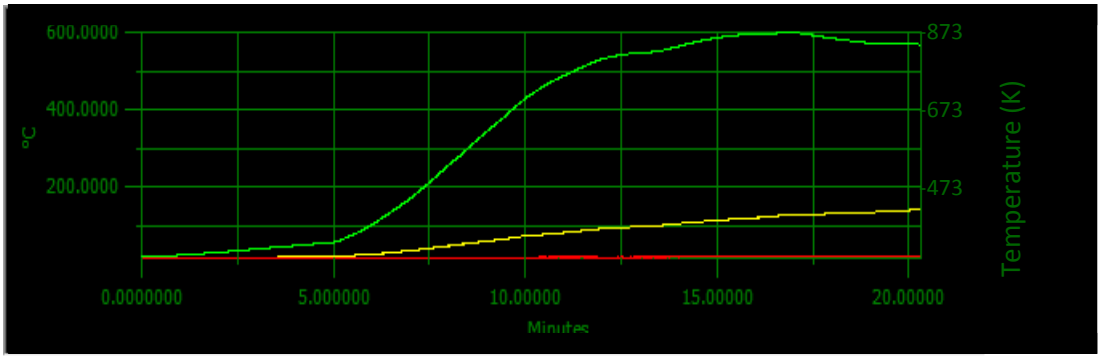

Figure 20: Experimental results

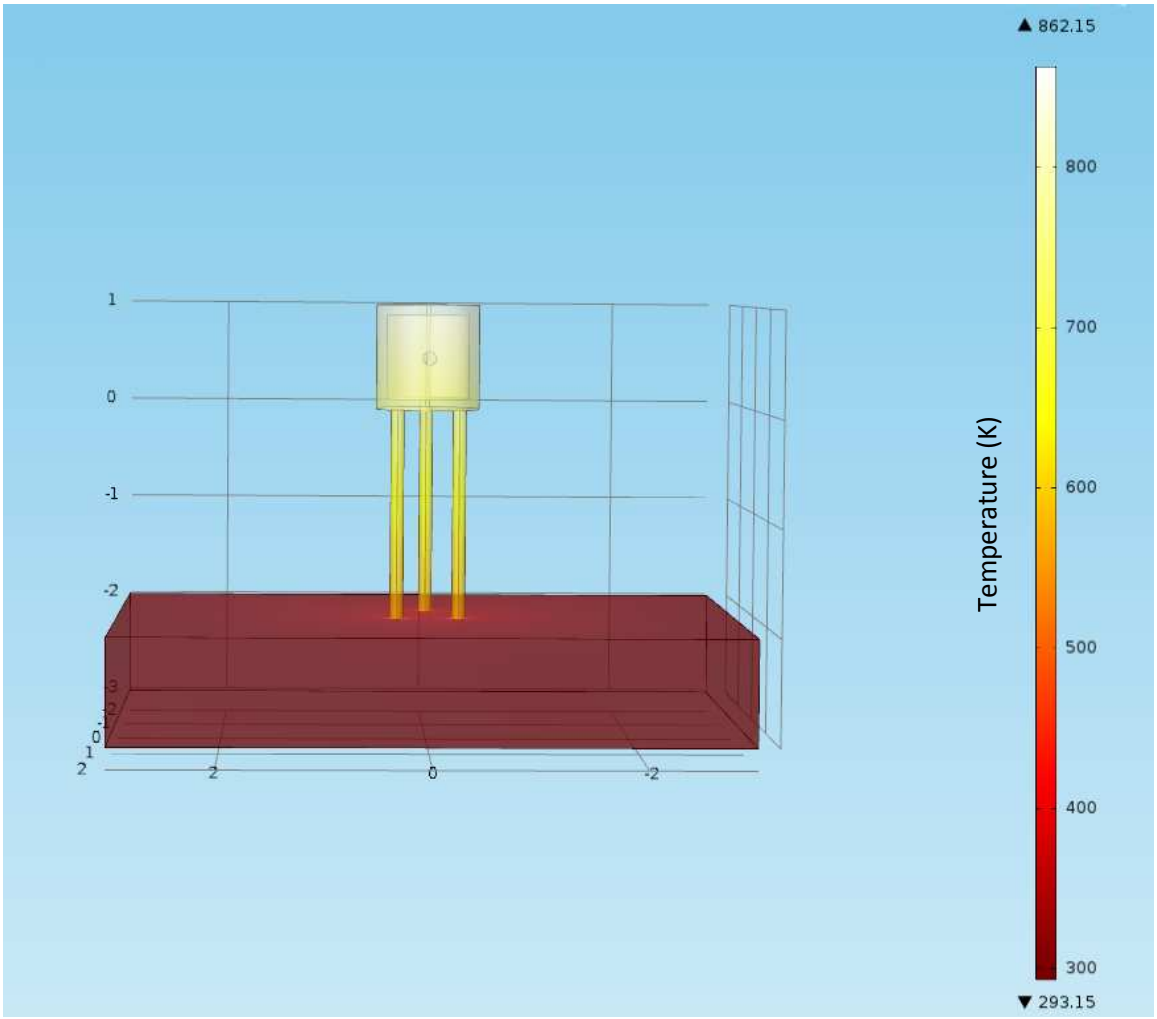

Figure 21: Computational results

Analyzing the two results shows that the maximum temperature of the experiment was 874.45 ± 1 K, and the maximum temperature of the computer model was 862.15 K, resulting in a difference of 12.3 ± 1 K.

3.5 Version 4.0

Maximum experimental temperatures were still below expectation. Drastic improvements to the mounting system were necessary. Having explored all the feasible leg configurations, the mounting system was redesigned by using tungsten wires as a support structure. The small diameter of the wires would limit the flow of heat while reducing the oxidizing insulation source. To achieve this, a steel brick was drilled with four holes. Small zirconia insulation beads with axial holes were inserted as legs into the holes, and tungsten wires threaded through them. The wires were crossed in the middle, and connected to the opposing legs. This crossing wire design created a "hammock" for the target to rest in during testing. Figure 22 shows the wire hammock concept.

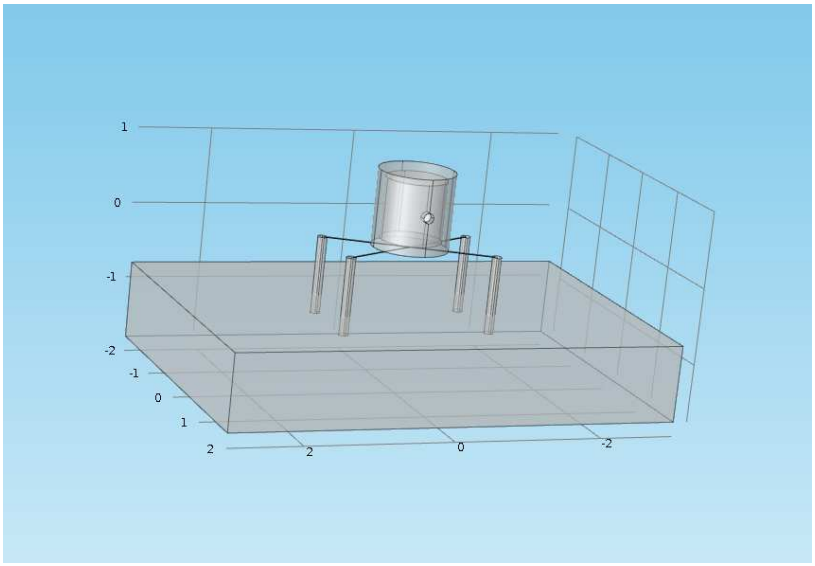

Figure 22: Computer model of "hammock" style mount

3.5.1 Testing Version 4.0

With the introduction of the hammock mount, the experimental temperatures rose to the highest found in testing, 963 K at the sample area. This was performed at 100 W power, which provided a power density over twice that of the plutonium fuel source. Even with the extra power, this temperature was significantly below the originally desired temperatures. However, without the inclusion of an emitter material that can retain a minimal emissivity at high temperatures, it may not be possible to reach the high temperatures desired by the theoretical design.

The pressure inside the vessel was reduced to ~30 mTorr and stayed relatively constant throughout testing. The surface finish of the material after testing was examined and found to largely maintain its reflectivity. Heating times were reduced to limit oxidation time as much as possible, instead of ramping up power over time maximum power was introduced at the beginning of the experiment. COMSOL models accurately predicted the outcome of the test, suggesting the model is accurate enough to use for RTPV design.

Using the more accurate 40 W power input, heating was performed three times to validate the performance of a PuO_2 loaded solid fuel cylinder. The temperature rose to a maximum level of 506 °C (779 K) and remained constant for the duration of the test. It was decided that given the available power densities and materials, design of the RTPV system must continue with the assumed maximum temperature of 779 K.

3.6 Issues Discovered

After exhausting all options for experimental variations, a few observations emerged that must be taken into account when designing or testing high temperature RTPV heat sources. Firstly, the emissivity of materials can vary with temperature. Specifically, in metals the

emissivity values can steadily rise. In selective emitters, the total emissivity will change as the peak of the corresponding blackbody curve passes in to the high emissivity region of the selective emitter emission spectrum. Keeping the emissivity down may not be possible, which would lead towards higher power densities and higher power to surface area ratios. Reflecting surfaces may be able to help reduce emissive losses by reflecting energy back at the source, but those options were not explored in this experiment.

Oxidation can heavily damage a metallic emitting surface, and effectively ruin optical insulation. Components that contain oxygen can cause damage even in a vacuum if in direct contact with a very hot surface. Oxides should be as dense as possible and resistant to breaking, shredding, or creating dust.

Thermal losses through the mounting structure are large and difficult to reduce. The most effective way to reduce thermal losses is by using wires in tension, as their small cross sectional area reduces conductive heat flow and their small radiating surface area reduced emissive losses.

3.7 Error Analysis

Because the experiment is being compared to computational models, the errors arise in the form of discrepancies between the test results and the modeling results. The computer models have been modified to represent the experimental data as close as possible, yet some difference in temperature readings still exists.

Experimental results were read with K-type thermocouples which were tested upon arrival in ambient lab conditions and a 273 K ice water bath. They were found to be accurate to $\pm$ 1 K. The model predicted near uniform heating around the target for almost all cases, yet during tests there was a much higher temperature at the laser impact point than the top of the

target. This difference varied in value depending on the power of the laser, but has a maximum difference of 150.05 ± 1 K. Because of the large difference, the impact point temperature was not used.

The computational model with the tungsten wire support assembly behaved well but had a large difference in maximum temperature of 89.23 ± 1 K, or ~11.5%. This was much larger than the results of the tantalum leg support of 12.3 ± 1 K. Temperatures of the final experimental test (Figure 23) and computational model (Figure 24) can be seen below.

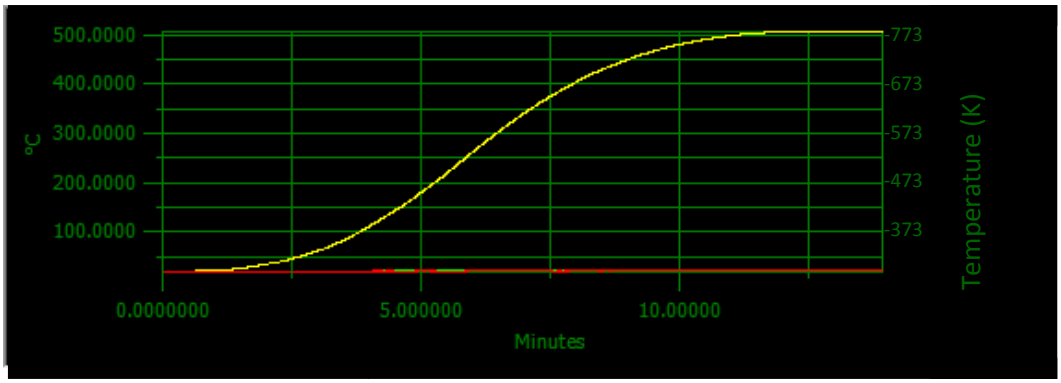

Figure 23: Max temp of wire-supported target

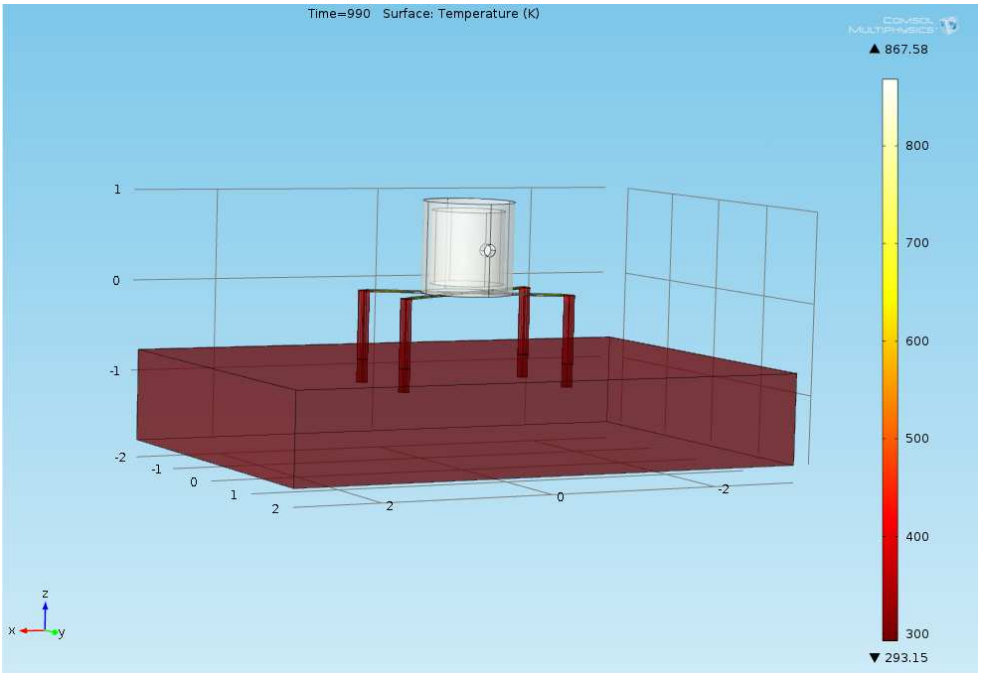

Figure 24: Max temp of computational model

The error between the model and the test is likely due to small variations from listed values in different material properties. The largest issue remains with the oxidation over time of the target, which can vary between tests based on temperature and duration. Even though an attempt was made to include this change, it is difficult to understand the precise effect on emissivity. If this is the case, use of the RTPV system in a vacuum should remove most of the oxidation and change the real world results to more closely match the model. Another factor could be the geometry of the final experimental setup, which includes bending wires and threaded beads, which are not accurately portrayed by the simple geometry of the model. This complex geometry will also not be present on the space-based RTPV system, which can be seen in the next chapter. Due to these factors which cause discrepancies between terrestrial and space-based RTPV uses, it was thought better to include the error and keep the current material properties rather than drastically change the properties to reduce error.

Chapter 4: Theoretical RTPV Design

4.0 RTPV Design Based on Experiment

The next step was to design an RTPV system based on the lessons learned from experimenting and the predictive abilities of the verified COMSOL models. Because the experimental testing was done with a specific sized fuel rod and 40 W thermal power, the theoretical design initially followed these criteria. A preliminary design of a 40 W thermal system can be seen in Figure 25.

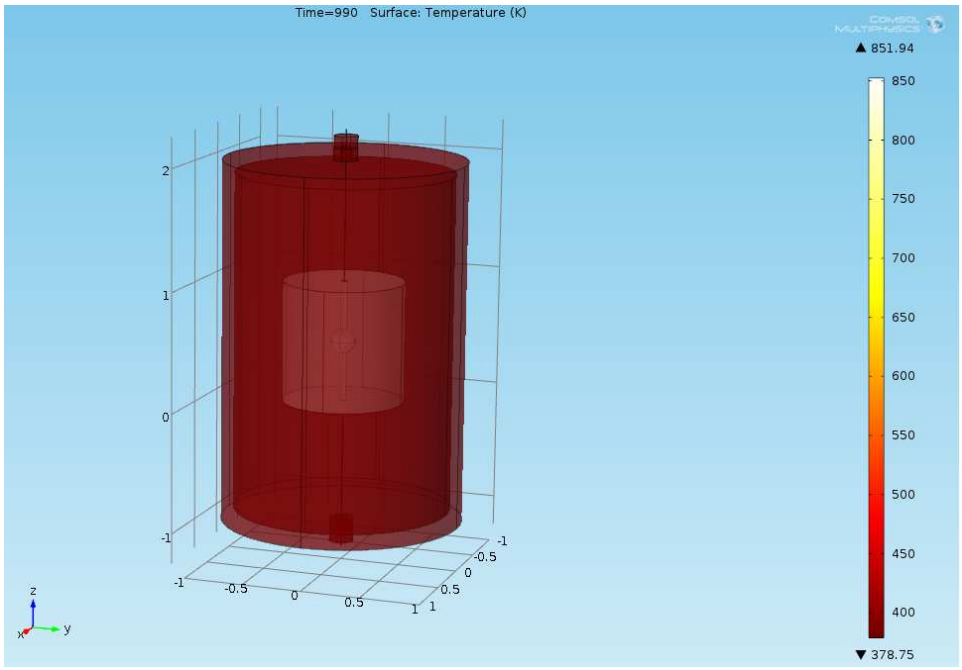

Figure 25: Initial RTPV theoretical design based off experiment

However, with the lower temperatures found from testing, the size of the system had to be increased to increase the power to surface area ratio and increase temperature. Because the testing was conducted with a tantalum target, tantalum was assumed to be layered on all reflective surfaces as optical insulation. The inside of the fuel would be a tungsten alloy CerMet

as previously planned. The emissivity profile was that of polished tantalum, assumed to be a gray body.

After preliminary calculations, it became apparent that a low power system would not be viable under these conditions because of the lack of temperature and the gray body emitter surface. The system had to be redesigned based on the abilities of the computational modeling given the materials used.

To determine the necessary size and temperatures of the theoretical system, it was deemed necessary that the efficiency must meet or exceed the efficiency of the current power production method of the MMRTG. That is to say, the efficiency must be at least 6%.

To make even the most infrared photovoltaic cells viable, the photon wavelengths must exceed at least 2μm. With InGaAs cells, the low end can reach 2.5 μm [32], with an average quantum efficiency of 0.65 for wavelengths between 1.8-2.5 μm. A few IR photovoltaic cell quantum efficiencies can be seen in Figure 26.

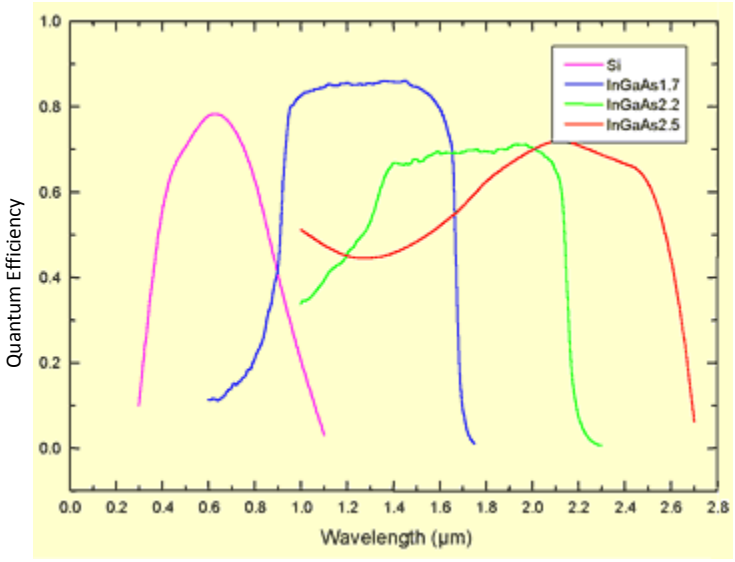

Figure 26: Quantum efficiencies of photovoltaic cells (InGaAs cells vary by dopant amounts) [32]

The conversion efficiency of InGaAs cells is seen in Figure 27. The plot shows that the efficiency increases as the wavelength of the photon increases, until reaching the minimum

band gap wavelength. Because each photon performs the same electron excitation and higher energy photons waste their excess energy, the minimum band gap energy photons are most efficient.

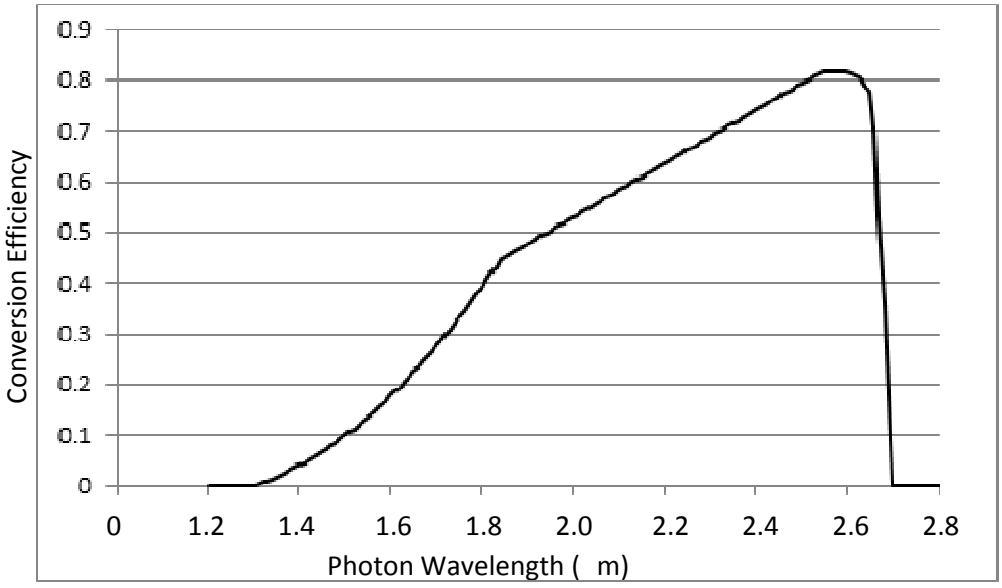

Figure 27: Example InGaAs conversion efficiency

Applying this trend to the InGaAs 2.5 cell determined an average conversion efficiency of 60%.

Of the total amount of power emitted, an estimated 10% would be lost to surface reflection of the PV cell [33] [34]. 65% of the remaining photons between 1.8 to 2.5 m would be absorbed, and 60% of that energy would be converted to electricity. With the shape of the emitted spectrum being similar to a blackbody, the fraction of emitted light in that range could be found by Table 3, below. To match the 6% efficiency of the MMRTG, 18% of the emitted light must be in that band, in order to have 65% of it absorbed at 60% efficiency.

Table 3: Fraction of area under blackbody curve correlated to wavelength times temperature [35]

Wavelength-Temperature Product, λT (μm*K)	Blackbody Fraction ($F_{0\rightarrow\lambda T}$)
600	9.29E-08
800	1.64E-05
1000	3.21E-04
1200	2.13E-03
1400	7.79E-03
1600	1.97E-02
1800	3.93E-02
2000	6.67E-02
2200	1.01E-01
2400	1.40E-01
2500	1.61E-01
2600	1.83E-01
2700	2.05E-01
2800	2.28E-01
2900	2.51E-01
3000	2.73E-01

Given that the λ values in question are 1.8μm and 2.5 μm, a temperature value must be found that when multiplied by those wavelengths had a difference in blackbody fraction of over 0.18. At a temperature of 1,200K, and λ of 1.8μm, the blackbody fraction was 0.094058. At a temperature of 1,200K, and λ of 2.5μm, the blackbody fraction was 0.27323, a difference of 0.17917. Therefore, the design temperature was set to 1,200 K to achieve a blackbody fraction as close to 18% as possible.

4.1 Geometry

The geometry of the system must be greatly increased from the original dimensions to allow for proper temperatures under these configurations. Figure 28 shows a design with all the

components listed.

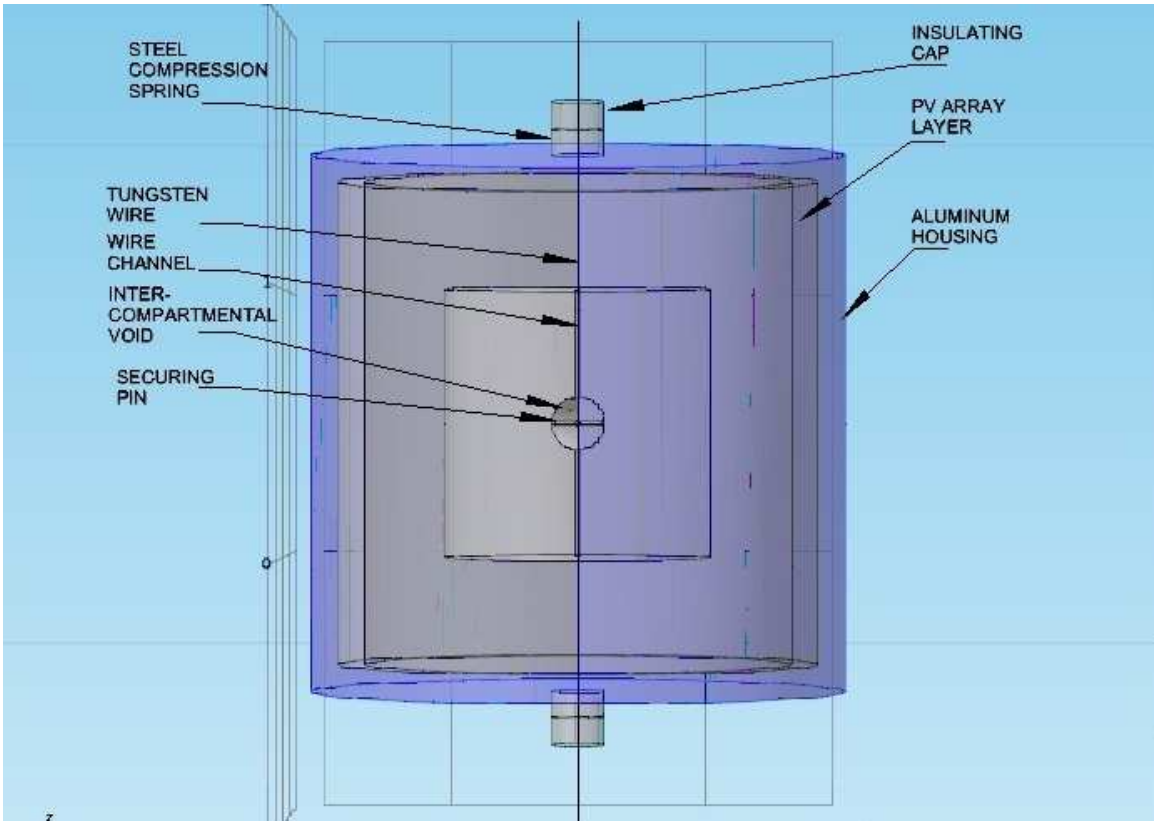

Figure 28: Labeled diagram of RTPV unit

While Figure 28 shows the assembly components, some dimensions must be changed to reach the desired temperature. Inside, a cylindrical fuel rod with dimensions of 8.13 cm diameter by 8.13 cm height produces 1 kW of thermal power. All sides of the rod are polished to reduce as much emissive loss as possible. With the assistance of spark plasma sintering, a small, spherical hole of 1.27 cm diameter can be placed inside the cylinder which is accessible by a 0.21 cm wide channel running through the axis of the cylinder. Threaded through this channel is a tungsten wire 0.104 cm diameter, which is attached to a securing pin equal in diameter to the wire. This beam is threaded into the fuel source with the wire until it reaches the internal cavity where it turns to be perpendicular to the run of the wire, holding the fuel rod in place.

The ends of the wire extend until reaching the housing, where they penetrate through the ends and are held taught by a spring/insulation assembly.

Inside the housing, the walls are lined with photovoltaic cells. The electrodes of the cells can pass freely through the walls of the housing and attach to circuitry as required. The aluminum housing is blackened on the outside surface to allow for maximum heat rejection.

4.2 Structural Analysis

To determine the geometry of the theoretical model, it had to be shown that the system could hold up to the stresses it will see during the mission. The most prominent of these stresses is the launch force. During a typical manned launch mission, astronauts are subjected to no more than three times earth's gravity [36]. This is due to the fact that excess forces can be fatal, and most astronauts are capable of still operating simple controls at these forces. Even though some unmanned launches may induce stronger forces, other components such as electronics or testing apparatuses can also limit how much force can be applied. Because of this, and the variation of forces, it was determined to analyze the structural capabilities based on the 3-G forces of a manned launch.

The weakest point in the assembly is the tungsten wire connecting the fuel rod to the external housing of the system. If that wire fails the entire system will stop functioning, and potentially melt through the housing. Similarly, if the support pin breaks under the weight of the fuel, the system will fail. It is important to size that wire correctly. Calculations were performed to determine the minimum diameter, and computational modeling software was used to verify the results. For a 1,000 W thermal fuel source, the CerMet matrix would have a mass of 6.219 kg.

The ultimate tensile strength of tungsten is given as 1,510 MPa [37]. However, the tensile strength will change as the system increases in temperature. The tensile strength at different temperatures is shown in Figure 29.

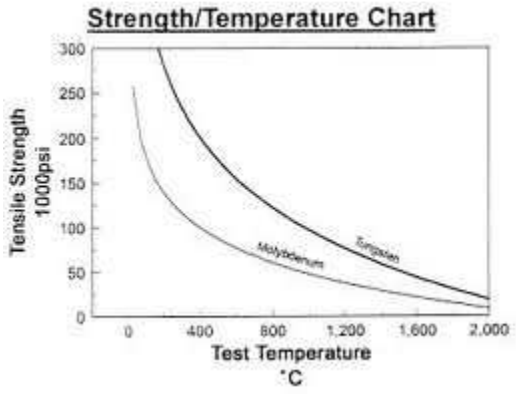

Figure 29: Tungsten tensile strength at different temperatures

At a temperature of 1,200K, the corresponding tensile strength of tungsten would be reduced to roughly 125,000 psi, or 862 MPa. To find the minimum acceptable diameter of the wire, Equation 4.1 is used, derived from the definition of stress being force per unit area.

$$d = 2 * \left(a * M * \frac{G}{TS * \pi}\right)^{.5} \quad [4.1]$$

Where d is the minimum diameter, *a* is the gravitational acceleration on earth, *M* is the mass of the solid fuel, *G* is the number of gravities applied, and *TS* is the maximum tensile strength. From this equation, the minimum wire diameter was found to be 0.52 mm. However, it is necessary to include a safety factor to ensure the wire does not break at all. Given the importance of the wire and the possibility of shaking or impact forces, it was decided that the diameter should be at least twice as wide as required. However, the wire must also thread through a channel in the fuel rod. Increasing the diameter naturally increases the volume of the

fuel without adding any increased power, which decreases the power density. With a safety factor of two, the final diameter was 1.04mm.

COMSOL was used to verify that the wire was sufficient to hold the mass of the fuel. A simple model was created of the wire with the support beam. One end anchored to the housing and one end was free, and the force of the mass was applied to the beam with the same assumption of a 3 G load. The results are shown in Figure 30.

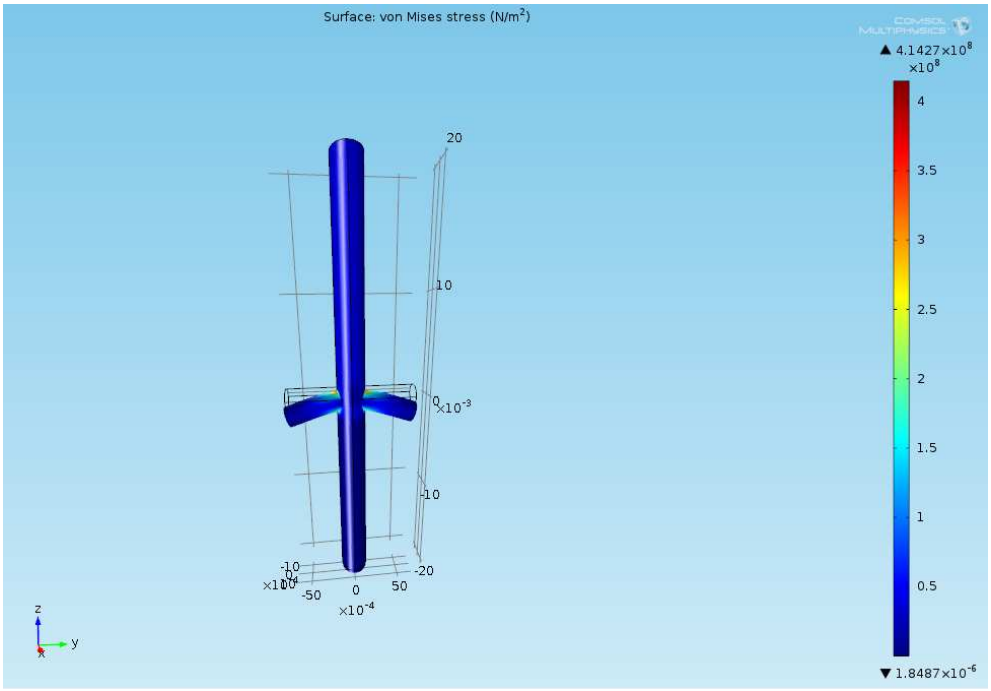

Figure 30: Center support wire of theoretical design under load

In Figure 30, it can be seen that the maximum stress of 4.143×10^8 Pa is smaller than the maximum tensile stress of 8.62×10^8 Pa, by almost exactly the safety factor of two. This configuration should support the fuel during launch and in conditions which have forces not exceeding three times earth's gravity.

4.3 Thermal Analysis

The model must also show that the theoretical system will be able to reach the temperatures required to emit the proper spectrum of light. The new model used the emissivity and heat transfer values found from the experimental setup, and the desired temperature was 1,200 K. The results of the initial COMSOL thermal analysis can be seen in Figure 31.

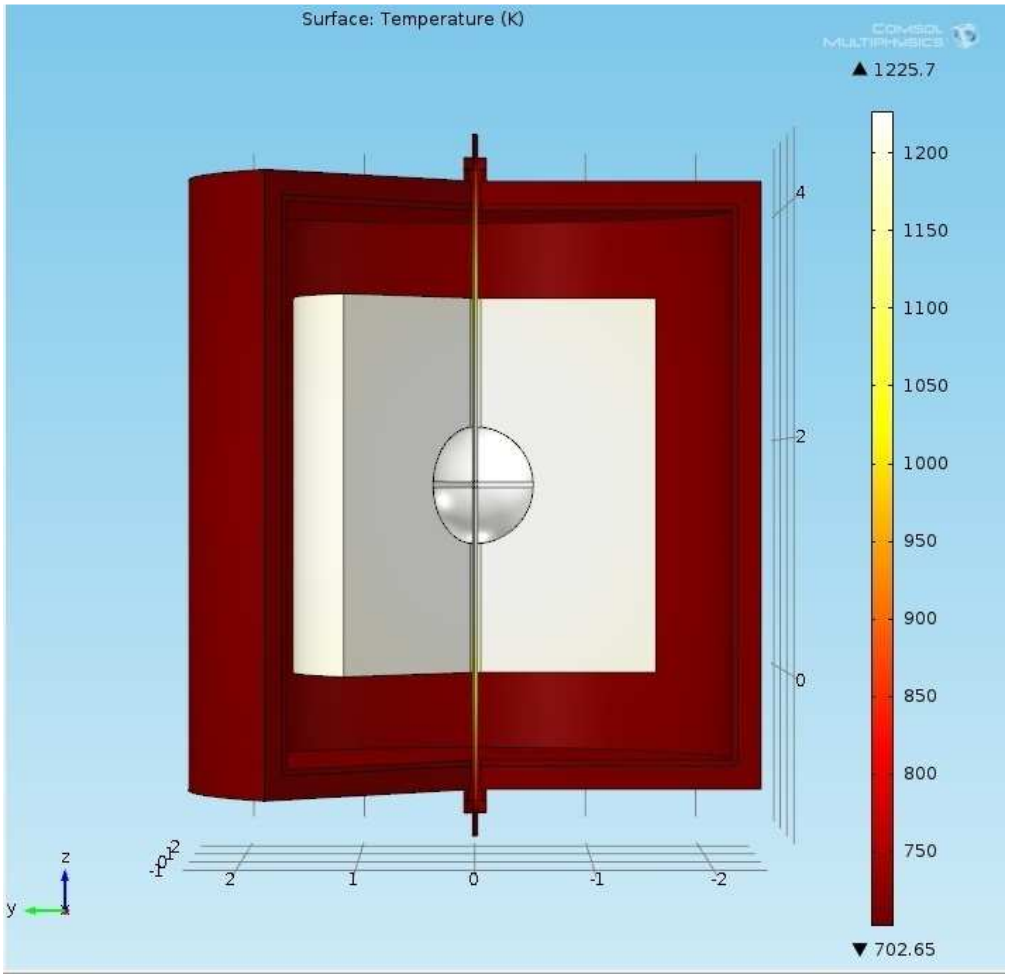

Figure 31: Initial thermal profile of theoretical design

While the design showed the proper temperature was achieved, it had failed reject heat through the exposed surface at a sufficient rate to keep the layer of photovoltaic cells below their maximum operating temperature of 353 K. Due to this, the design would require radiators

to reject the excess heat, or a mounting system that did not rely on radiative cooling. This could be achieved by placing the RTPV system inside a larger housing or on the ground, or anything that could maintain a constant, cooler temperature. Figure 32 shows the effects of wall cooling on the system, and the slight decrease in maximum temperature.

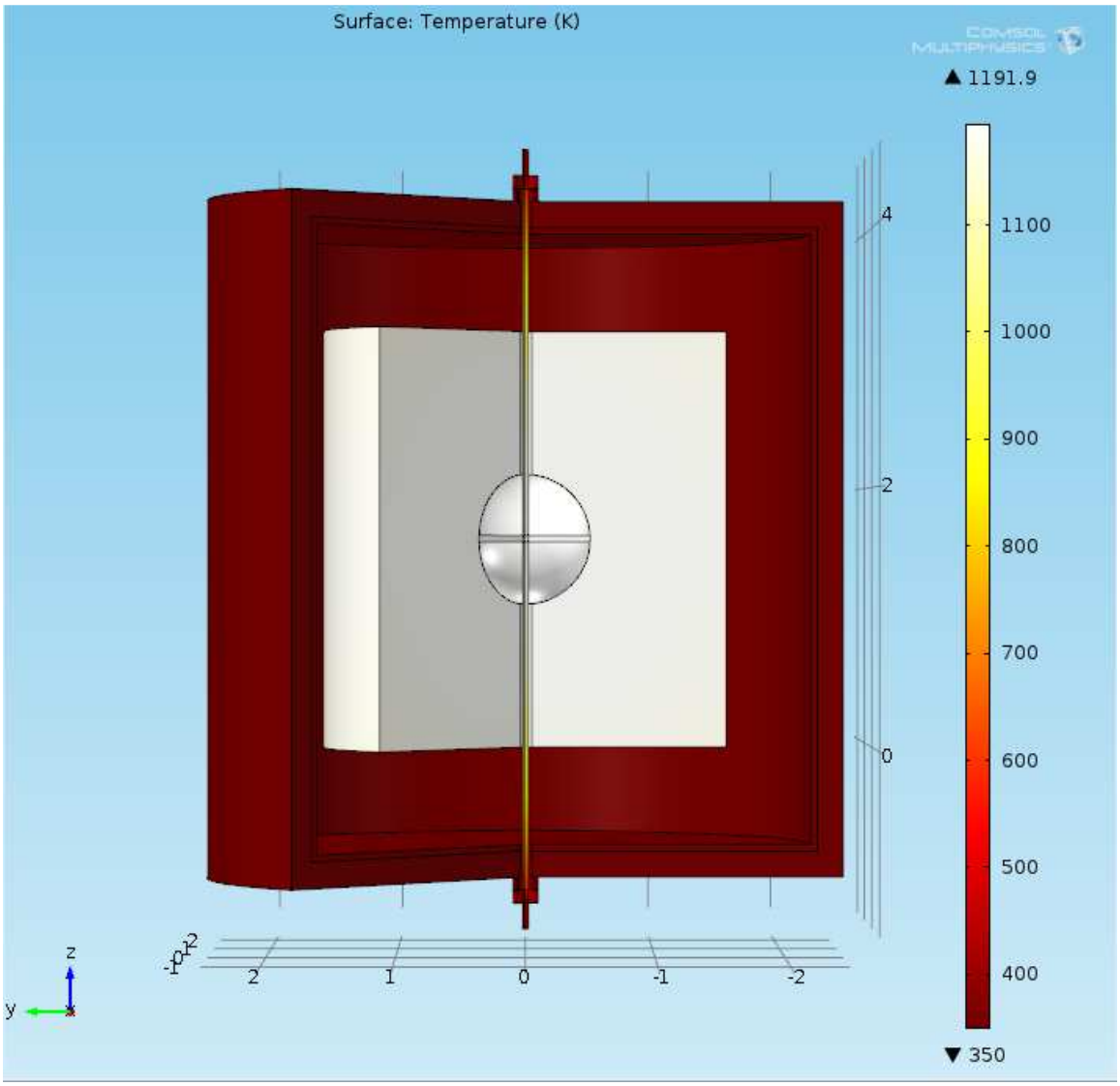

Figure 32: RTPV model with cooling

With the addition of a heat rejection system, extra mass would also be added. By solving Equation 2.2 for the area, and assuming a blackbody surface with an emissivity of one, in order to reject 940 W the radiator would need to have an area of 1.105 square meters. A usual

radiator has a mass of 5-10 kg/m^2 [38] [39]. That means this system would need between 5.5-11 kg of radiator mass added. The total mass of the fuel and the housing in this situation is 10.65 kg; with the addition of 11kg of radiators in a worst-case scenario, that makes the whole system mass 21.65 kg with an electrical production of 60 W. That equates to 360.8 kg/kW. Comparatively, the current MMRTG produces 120 W of electrical power and has a mass of 43 kg. The MMRTG power ratio is then 358.3 kg/kW. This value is extremely close to the new RTPV design, in the worst-case scenario.

Chapter 5: Conclusion

With the experimental system functioning, certain RTPV aspects can be measured to empirically determine their performance capabilities and usefulness in an RTPV system. Emissivity, thermal conductivity and configuration all have important effects on RTPV system design. In the case of a polished tantalum emitter, surface emissivities change so much with temperature that the system needs to be quite large to remain viable. Additionally thermal losses and oxidation can ruin an RTPV system. Being able to test these aspects in the laboratory provides useful insight into the development of the project. With the capabilities of the experimental setup other surface emitters can now be tested and modeled in order to create a high efficiency RTPV system.

The theoretical model shows that even with a non-optimal emitter and heavy radiators, the RTPV system can compete with the current power production methods. This can be improved further by increasing efficiency and reducing radiator mass. Testing and modeling new configurations will allow for RTPV power sources to surpass current methods and provide power to far reaching space systems for decades.

References:

[1] Chubb, D., *Fundamentals of Thermophotovoltaic Energy Conversion,* Elsevier Science, 2007

[2] Elison Matioli, et al., *High internal and external quantum efficiency InGaN/GaN solar cells,* Applied Physics Letters, January 10th, 2011

[3] Seal, M., *Viking 29 – A Thermophotovoltaic Hybrid Vehicle Designed and Built at Western Washington University,* SAE Technical Paper 972650, 1997

[4] Guazzoni, G. *A, Retrospective of Four Decades of Military Interest in Thermophotovoltaics*, AIP Conference, 2004

[5] Shor, R. et al, *Strontium-90 Heat Sources*, Oak Ridge National Laboratory, May 1971

[6] Shultis, J. K., and Faw, R. E., *Fundamentals of nuclear science and engineering*, CRC Press, 2002.

[7] American Nuclear Society (ANS), *MMRTG,* http://anstd.ans.org, Nov 5th, 2013

[8] Turns, S., *Thermal-fluid sciences, an Integrated Approach,* Cambridge University Press, 2006

[9] NASA, *Radioisotope power systems,* http://solarsystem.nasa.gov/rps/types.cfm 2013, Nov 5th, 2013

[10] American Nuclear Society (ANS) *GPHS-RTG* http://anstd.ans.org, Nov 5th, 2013

[11] American Nuclear Society (ANS) *ASRG* http://anstd.ans.org, Nov 5th, 2013

[12] Cengel, Y., Boles, M. *Thermodynamics, An Engineering Approach. 6th edition.*, McGraw-Hill, 2008

[13] Shaltins, R., Wong, W., *Advanced Stirling Technology Development at NASA Glenn Research Center,* NSTC Conference 2007

[14] NASA, *Advanced Radioisotope Power Systems Report,* D-20757, NASA JPL, 2001

[15] L. C. Olsen, P. Cabauy and B. J. Elkind, *Betavoltaic Power Sources*, Physics Today 65, No. 12, 35 (December 2012).

[16] Davis, J., *Waste to Energy Evaluation: US Virgin Islands*, National Renewable Energy Laboratory, August 2011

[17] Cubesat, *Cubesat in the news,* http://www.cubesat.org/, Dec 10th, 2013

[18] Chubb, D. Wolford, D. S., *Theoretical Performance of a Radioisotope Thermophotovoltaic (RTPV) power system,* 7th International Energy Conversion Engineering Conference, 2009

[19] Home, W. D. et al., *Performance tuned radioisotope thermophotovoltaic space power system,* The American Institute of Physics, 1-56396-747-2, 1998

[20] Schock, A. et al., *Small Radioisotope Thermophotovoltaic (RTPV) Generators,* American Institute of Physics, 1996

[21] General Atomics Research Staff, *General Atomics RTPV Presentation*, Personal Meeting, April 2012

[22] Joannopoulos, J. D. et al., *Photonic Crystals Molding the Flow of Light,* Princeton University Press, 2008

[23] Rinnerbauer, V. *Large-area fabrication of high aspect ratio tantalum photonic crystals for high-temperature selective emitters,* American Vacuum Society, 2012

[24] Wilt, D. M. et al., *High efficiency indium gallium arsenide photovoltaic devices for thermophotovoltaic power systems,* Applied Physics, May 1994

[25] Li, G., Li, G., Neumark, J. F., *Investigation of ZnSe for ZnSe/GaAs/Ge High Efficiency Solar Cells,* Proceedings of the 13th Workshop on Quantum Solar Energy Conversion - (QUANTSOL 2001) March 11-17, 2001, Kirchberg in Tirol, Österreich

[26] Baum, E. *Chart of Nuclides Sixteenth Edition,* KAPL 2002

[27] Purves et al., *Life: The Science of Biology*, 4th Edition, Sinauer Associates, W.H Freeman and Company, 2006

[28] Iles, P. *Photovoltaic Principles Used in Thermophotovoltaic Generator,* American Institute of Physics, 1995

[29] Sunpowercorp, *Sunpower E19/318 information manual*, document #001-42188, 2009

[30] Duffie, J., Beckman, W.*, Solar Engineering of Thermal Processes*, Wiley and Sons, 1980

[31] Thorlabs *Thorlabs – Zinc Selenide (ZnSe) Windows,* http://www.thorlabs.us/newgrouppage9.cfm?objectgroup_id=3981, Nov 5th, 2013

[32] Sensors, Inc., *What is InGaAs?,* http://www.sensorsinc.com/GaAs.html, Nov 5th, 2013

[33] PerkinElmer Inc, *Reflectance Measurements of Materials Used in the Solar Industry,* PerkinElmer, 2009

[34] Australian National University, *Analysis and Optimization of Silicon Solar Cell Front Surface Optics,* ANU, 2009

[35] Howell, J. R. et al., *Thermal Radiation Heat Transfer, fifth edition,* CRC Press, 2011

[36] Shaw, T.L., et al., *Simulation of Shuttle Launch G Forces and Acoustic Loads Using the NASA Ames Research Center 20G Centrifuge,* NASA Ames Research Center, 1994

[37] Budynas, R., *Advanced Strength and Applied Stress Analysis*, McGraw-Hill, 1999

[38] Techbriefs.com, *Lightweight Carbon-Carbon High-Temperature Space Radiator,* http://www.techbriefs.com/component/content/article/3156, November 5th, 2013

[39] NSS.org, *Thermal management in Space,* http://www.nss.org/settlement/nasa/spaceresvol2/thermalmanagement.html November 5th, 2013